SANDIA REPORT

SAND87–2118 • UC–32
Unlimited Release
Printed October 1987

Ducted Propeller Design and Analysis

Robert J. Weir

Prepared by
Sandia National Laboratories
Albuquerque, New Mexico 87185 and Livermore, California 94550
for the United States Department of Energy
under Contract DE-AC04-76DP00789

Abstract

The theory and implementation of the design of a ducted propeller blade are presented and discussed. Straightener (anti-torque) vane design is also discussed. Comparisons are made to an existing propeller design and the results and performance of two example propeller blades are given. The inflow velocity at the propeller plane is given special attention and two dimensionless parameters independent of RPM are discussed. Errors in off-design performance are also investigated.

SF2900Q(8-81)

Issued by Sandia National Laboratories, operated for the United States Department of Energy by Sandia Corporation.

Printed in the United States of America
Available from
National Technical Information Service
U.S. Department of Commerce
5285 Port Royal Road
Springfield, VA 22161

NTIS price codes
Printed copy: A04
Microfiche copy: A01

Contents

List of Figures

Symbols

A	area (unsubscripted refers to annular area swept out by the propeller blades)
A_1	thrust distribution exponent
B	number of blades (unsubscripted refers to propeller)
C	nondimensional force coefficient$=\frac{F}{q}$
c	chord
D	drag
F	force
j	local advance ratio$=\frac{V}{\Omega r}$
j'	radial advance ratio$=\frac{Vr}{\Omega R^2}$
K	propeller induced velocity factor
L	lift
P	input power
Q	torque
q	dynamic pressure$=\frac{1}{2}\rho V^2$ (unsubscripted refers to freestream)
R	propeller tip radius
r	radial position along blade span
s	duct length to exit radius ratio
z	duct airfoil cross section camber ratio (maximum camber/chord)
T	thrust
V	air velocity
w	velocity difference between freestream and propeller jet velocities $= V_0 - V_4$
x	fraction of blade span$=\frac{r}{R}$
α	angle of attack (unsubscripted refers to a propeller section)

β	pitch angle setting (unsubscripted refers to the propeller)
δ	duct induced velocity factor
θ	angle from axial flow line to velocity vector behind the propeller
ρ	air density
σ	ratio of clear duct area to propeller swept area=$\frac{A_t}{A}$
ϕ	angle from propeller plane to resultant velocity vector into the propeller
ψ	angle from straightener vane trailing edge camber line to axial flow line
Ω	propeller angular velocity
ω	jet swirl angular velocity

subscripts

0	freestream
4	jet
A	axial flow at the propeller plane
D	drag
d	duct induced (C_d refers to sectional drag)
H	hub
i	propeller induced
L	lift
l	sectional lift
P	propeller
R	resultant vector
T	thrust (V_T refers to propeller tip velocity)
V	straightener vane
X	force tangent to the propeller plane of rotation
Y	force normal to the propeller plane of rotation

1 Introduction

The use of ducted propellers as the main propulsion units on aircraft has been investigated since the end of World War II. Because, theoretically, a ducted propeller is more efficient in hover than a free propeller, it is desirable for Vertical Take Off and Landing (VTOL) applications. However, losses involving friction and boundary layer separation inside the duct often decrease the efficiency gain. Besides fluid losses, the weight of the duct often negates any benefit it provides. This problem can be partially alleviated by using strong, lightweight composite materials and integrating the duct into the structure.

Crucial to the performance of a ducted propeller is the design of the propeller itself. A method of designing a ducted propeller blade was investigated and developed to maximize the thrusting efficiency for the Airborne Remotely Operated Device (AROD); a VTOL surveillance platform being developed for the United States Marine Corps. This method is based on Blade Element Theory, commonly used in free propeller design, but uses an approach to the propeller-duct interaction proposed by T. W. Sheehy[1].

2 Discussion

The effects of the duct on the propeller are two-fold: 1) inducing an increment of velocity, $\Delta V = V_0\delta$, through the propeller in forward motion, and 2) negating tip effects if the gap between the inner wall and the propeller tip is very small (i.e. 0.03 in.). This small gap was assumed in the analysis.

2.1 Inlet Velocity

From momentum, the thrust of a ducted propeller is the product of the mass flow rate, $\dot{m}$, and its change in velocity. Expressing the change in velocity as w and noting, from McCormick[2], that half of the velocity change occurs upstream of the propeller and including the increment in velocity induced by the ducted propeller in forward motion, then the velocity through the propeller, the thrust, and the thrust coefficient are;

$$V_A = V_0 + \frac{w}{2} + V_0\delta \tag{1}$$

$$T = \dot{m}w = \rho A V_A w = \rho A \left(V_0 + \tfrac{w}{2} + V_0\delta\right) w$$

$$C_T = \frac{T}{qA} = 2\left(1 + \frac{w}{2V_0} + \delta\right)\frac{w}{V_0} \tag{2}$$

where

δ is the factor to determine the duct induced velocity into the propeller in forward motion
$w = V_4 - V_0$
V_4 is the propeller jet velocity (velocity in the jet far downstream of the propeller)
V_0 is the freestream velocity
T is the total thrust
q is the dynamic pressure $= \frac{1}{2}\rho V_0^2$
ρ is the air density
A is the annular area swept out by the propeller blades$= \pi\left(R^2 - R_H^2\right)$
R is the propeller radius
R_H is the hub radius

The thrust coefficient for a free propeller (no duct induced velocity) is

$$C_{T_P} = 2\left(1 + \frac{w}{2V_0}\right)\frac{w}{V_0} \tag{3}$$

So, the difference in C_T between the ducted propeller and the free propeller is

$$\Delta C_T = 2\delta\left(\sqrt{1 + C_{T_P}} - 1\right) \tag{4}$$

Solving for w in equation (3) yields

$$w = V_0\left(\sqrt{1 + C_{T_P}} - 1\right) \tag{5}$$

2.1.1 Duct Induced Velocity

Finding the increment of velocity induced by the duct in forward flight is accomplished by using the relation developed by Helmbold[3] a length to exit radius ratio, s, between 0.5 and 2.0 and a camber ratio, z (the ratio of the maximum difference between the duct mean camber line and the chord line to the duct chord length), between 0.05 and 0.1. For these values, the velocity induced by the duct in forward flight can be expressed as

$$\delta_d = 1 - \left(\frac{R_e}{R}\right)^{\frac{1}{2}}\left(\frac{0.458 + 4.431s}{1 + 1.089s}z + \frac{2.033 + 4.88s}{1 + 0.893s}sz^2\right) \tag{6}$$

where R_e is the duct exit radius.

The paper by T. W. Sheehy gives a relation for the duct induced velocity which is the negative of equation (6). This, however, resulted in the propeller thrust coefficient,C_{T_P}, being double the thrust coefficient of the propeller and the duct combined. This would imply that ducting the propeller is inherently detrimental, which contradicts past conclusions that ducting the propeller is beneficial, if the duct weight can be held low. The above modified expression resulted in the propeller providing about half of the total thrust, which is the prediction of the momentum analysis done by Lazareff[4]. The conclusion is that Sheehy's statement of Helmbold's relation is in error and that equation (6) is correct.

2.1.2 Propeller Induced Velocity

Since there is an energy source in the duct, namely the propeller, there is another duct induced velocity due to the interaction of the duct and that source in forward motion. Kucheman and Weber[5] provide the following expression for the propeller induced velocity term, δ_i;

$$\delta_i = K\left(\sqrt{1+C_{T_P}}-1\right) \tag{7}$$

where the value of K depends on the geometry of the shroud and the position of the propeller in the duct. The total duct induced velocity, $V_0\delta$, in forward flight is then the sum of $V_0\delta_d$ and $V_0\delta_i$.

2.1.3 Induced Velocity in Hover

In hover, there is no V_0, so C_T is based on V_A instead of V_0

$$C_T = \frac{T}{\frac{1}{2}\rho V_A^2 A} \tag{8}$$

If the expansion is complete at the exit, denoted by subscript e,

$$V_4 = V_e$$

$$T = \dot{m}V_e = \rho A V_A V_e$$

and from the conservation of mass,

$$V_e = \frac{AV_A}{A_e} = \frac{V_A}{\sigma}$$

then

$$V_A = \sqrt{\frac{T\sigma}{\rho\pi\left(R^2-R_H^2\right)}} \tag{9}$$

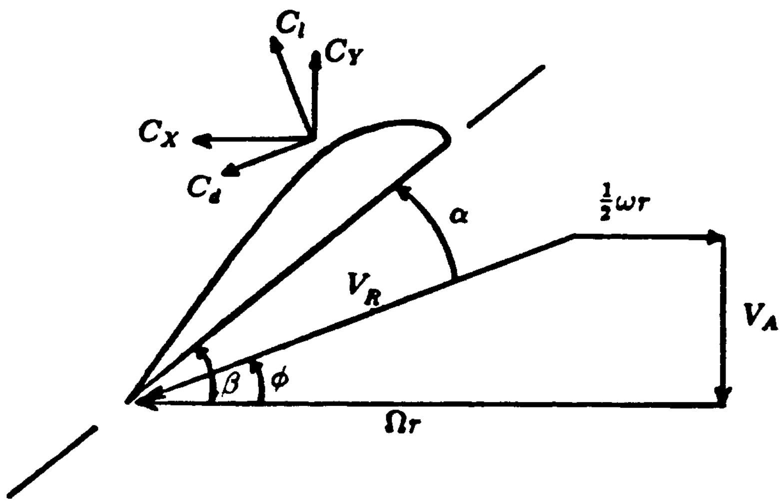

Figure 1: Propeller Blade Sectional Geometry

where R_H is the hub radius and σ is the exit area to propeller area ratio. Thus V_A in hover is dependent only on the desired hover thrust, air density, propeller size, and the duct expansion. This then becomes the value of the velocity V_A through the propeller when in hover. The final values of δ, C_T, C_{T_P}, and V_A are found by iterating on equations (1) through (7) if in axial flight, or (3) through (9) if in hover.

2.2 Blade Design by Blade Element Theory

The analysis leading to the propeller design is based on blade element theory. At each station along the span of the propeller blade, the airfoil section at that station generates lift and drag according to its sectional properties; C_l and C_d, the air velocity V_R, and the blade pitch setting angle β (see Figure 1). The air velocity is composed of the axial velocity V_A, the rotational velocity Ωr, and half of the final swirl velocity $\frac{1}{2}\omega r$ (half is induced upstream of the propeller and half in the slip stream).

2.2.1 Swirl Velocity Induced by the Propeller

The swirl velocity is induced by the rotating propeller blade dragging some of the air it passes through along with it. This velocity can be expressed, from Pope[6], and the relation for the factor e in Pope's equation, $e = \frac{\omega r}{V_A}$, as;

$$\frac{1}{2}\omega r = \frac{P}{2r\Omega\rho V_A A} \tag{10}$$

where

P is the power input into the air by the propeller$= \frac{1}{2}T_P V_A$
T_P is the thrust provided by the propeller
r is the radial station from the hub center
Ω is the propeller angular velocity

After $\frac{1}{2}\omega r$ is determined, ϕ can be determined trigonometrically (see Figure 1).

2.2.2 Determination of Forces on the Blade Elements

The vertical and horizontal force components on the blade element are;

$$C_Y = C_l\left(\cos\phi - \frac{D}{L}\sin\phi\right) \tag{11}$$

$$C_X = C_l\left(\sin\phi + \frac{D}{L}\cos\phi\right) \tag{12}$$

This indicates that, for high ratios of thrust to engine torque, the lift to drag ratio $\left(\frac{L}{D}\right)$ should be maximized. Maximizing $\frac{L}{D}$ then determines what angle of attack, α, the local airfoil section should have during operation to maximize the propeller efficiency. Since, from Figure 1, the sectional angle of attack is the difference between the air velocity angle, ϕ, and the blade pitch angle, β, the most efficient angle of attack of the section can be achieved by selecting the correct β for that section at its design operating condition.

2.2.3 Chord Distribution Determined by Thrust Distribution

The incremental thrust from each blade element is given by;

$$dT_P = BcC_Y q_R R dx$$

so that the local blade chord at radial station r is;

$$c = \frac{\frac{dT_P}{dx}}{BRC_Y q_R} \tag{13}$$

where

B is the number of blades
$q_R = \frac{1}{2}\rho V_R^2$
$x = \frac{r}{R}$

The thrust distribution over the blade, $\frac{dT_P}{dx}$, can be varied to yield the chord distribution necessary to produce a given thrust with maximum root chord restrictions. The present analysis uses a relation for the thrust distribution which is an exponential function of the blade radial station only;

$$\frac{dT_P}{dx} \sim \left(\frac{x}{x_H}\right)^{A_1} \tag{14}$$

where x_H is x at the hub and A_1 is first assumed, then modified during iterative passes on the propeller chord distribution. This relation was chosen because it is simple and easy to modify, yet very flexible with a wide range of possible thrust distributions. The propeller design after each iteration is checked for the thrust produced over the blade. This thrust is multiplied by the number of blades and the ratio of the total thrust coefficient to the propeller thrust coefficient, $\left(\frac{C_T}{C_{T_P}}\right)$, to arrive at the total thrust. If this thrust is different from the required thrust, A_1 is multiplied by the ratio of the old thrust to the new thrust and that value is reiterated on until a value of A_1 is found which will accommodate both the total thrust and the ratio of the total thrust to that of the propeller.

2.3 Flow Straightener Design by Element Torque Matching

Flow straightener vanes can be included in the analysis as well. The flow straightener vanes need accomplish two tasks: turn the flow after it leaves the propeller so that it leaves the duct flowing axially (i. e. taking out the swirl velocity) and counter the torque produced by the forces on the propeller in the plane of rotation. The first is accomplished by choosing the vane airfoil cross section at each station to have a mean camber line at the trailing edge whose tangent is parallel to the axial flow line. The second is accomplished by equating the torque of each blade section on each blade to the torque generated by the straightener vane sections directly downstream of the blade sections.

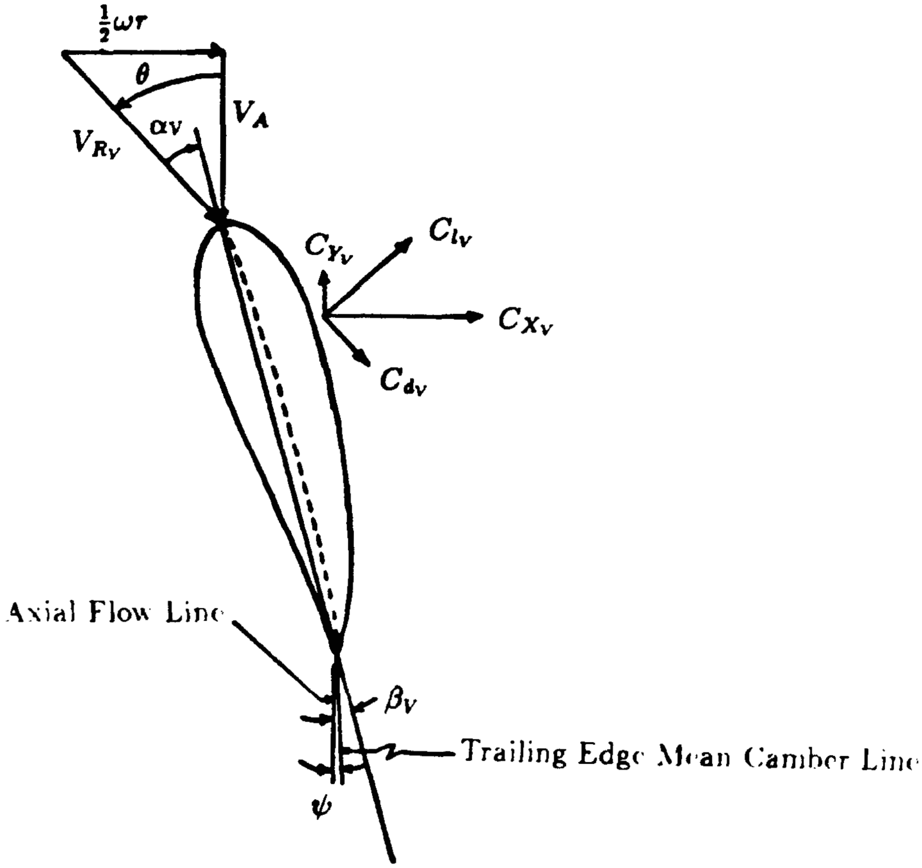

Figure 2: Straightener Vane Sectional Geometry

2.3.1 No Swirl Condition

To provide purely axial flow, the swirl velocity from the propeller must be negated. This is done by requiring that the mean camber line of the trailing edge of the vane be as nearly parallel to axial flow as is practical, i. e. $\psi \to 0$ (see Figure 2), since thin airfoil theory states that the flow will follow the mean chamber line of the airfoil.

2.3.2 Vane Chord Distribution Determined by Equating Element Torques

The flow straightener vanes can be simultaneously designed to take out the torque on the vehicle produced by the propeller and the engine. The incremental torque generated by each propeller blade element is;

$$dQ = BcC_X q_R R^2 x dx$$

To counter this torque, an element of the straightener vanes of the same width and at the same radial station must generate the same torque as that produced by the propeller blade element, but in the opposite direction. The torque generated by a vane element (denoted by the subscript v) is;

$$dQ_v = B_v c_v C_{X_v} q_{R_v} R^2 x dx$$

Equating the two and noting that V_A is the same for the propeller as it is for the vanes, yields;

$$c_v = \frac{B c C_X \cos^2\theta}{B_v C_{X_v} \sin^2\phi} \tag{15}$$

2.3.3 Determination of the Forces on the Vane Elements

The vertical and horizontal force components on the straightener vanes are determined like those on the propeller and are;

$$C_{Y_v} = C_{l_v}\left(\sin\theta - \frac{D_v}{L_v}\cos\theta\right) \tag{16}$$

$$C_{X_v} = C_{l_v}\left(\cos\theta + \frac{D_v}{L_v}\sin\theta\right) \tag{17}$$

The vertical force component on the vanes then contributes to the thrust. This should be taken into account by reducing the required duct-propeller thrust and recalculating the propeller required for such a reduced thrust. This is then iterated on until the total vertical force component on the duct-propeller combination balances the required thrust.

3 Verification

To verify this analysis, the propeller blade section, required thrust, RPM, and duct conditions were taken for a vehicle designed by Convair[7]. The propeller blade derived by the computer was then compared to the actual seven-foot diameter Convair propeller blade. The Convair propeller was 3-bladed, used a NACA 16-512 airfoil section at an L/D of 67, rotated at 1860 RPM to produce 2200 lbs of thrust, and consumed 400 hp on a sea level standard day with no duct diffusion considered. The NACA 16-512 has an L/D of 67 at angles of attack of 4° and 8°. It is stated that the blade angle of attack is far from stall to increase off-design performance, so the angle of attack of each blade element is fixed at 4° which has a C_l of 0.7.

Figures 3 and 4 show the comparison between the design of a propeller with a 7-foot diameter by the present analysis and Convair's 7-foot diameter propeller. The agreement is very good with the propeller chord distribution being, at most, 2% lower than Convair's chord at any location. The propeller pitch distribution shows almost the same accuracy with at most a 6% greater pitch angle than that used by Convair. The predicted power consumption also compares well with 411 hp to Convair's 400 hp.

4 Design Examples

4.1 Constraints

The examples which follow were done in support of the AROD project for the Marines. The duct geometry was for a propeller diameter of 2 ft, hub diameter of 8 in, an exit radius of 1.14 ft reflecting a diffuser total angle of 14°, and duct length to exit diameter and camber ratios of 1.24 and 0.1, respectively, see Figure 5. This geometry resulted in an exit to propeller plane area ratio of 1.34.

The propeller blades were restricted to 3 in number and had to produce a total duct-propeller thrust of 85 lbs in hover at 7200 RPM in an air density of $0.00192\frac{slugs}{ft^3}$. Two blade sections were considered; the NACA 4312 and the Gö 610 airfoils. The propeller maximum root chord was limited by two constraints. The vertical distance between the leading and trailing edges of the propeller at the root could not exceed 2 in. and the cross-sectional area of the root section could not be less than the 0.6 in^2 of fiber from the hub attachment for the composite blade. Areas of 0.71 and 0.75 in^2 for the NACA 4312 and Gö 610 , respectively, were used to leave room for the resin matrix.

4.2 NACA 4312 Blade

Figure 6 shows the predicted thrust distributions over the propeller radius for the two airfoil sections. The NACA 4312 airfoil is similar to the popular propeller airfoil, the Clark Y. Though 3-dimensional data were available, none of the needed 2-dimensional data for the Clark Y airfoil were found. The maximum L/D for this airfoil is 80 and occurs at an angle of attack of 10° where the C_l is 0.8. To account for the losses at the tips and to be conservative, the lift was reduced and the drag increased by 10% so that $C_L = 0.72$ and L/D= 66.12. The resulting propeller, for a thrust of 85 lbs, has a blade taper ratio (the ratio of blade root chord to blade tip chord) of 2.61, a root blade pitch angle of 41.98°, and a tip blade pitch angle of 21.01°. The torque necessary to rotate the propeller at 7200 RPM is 10.23 ft-lbs. This results in an engine power setting of 14.02 hp, resulting in a propulsive efficiency (thrust power/torque power) of 92.4%. The design propeller geometry is shown in Figure 7 and the pitch distribution is shown in Figure 8.

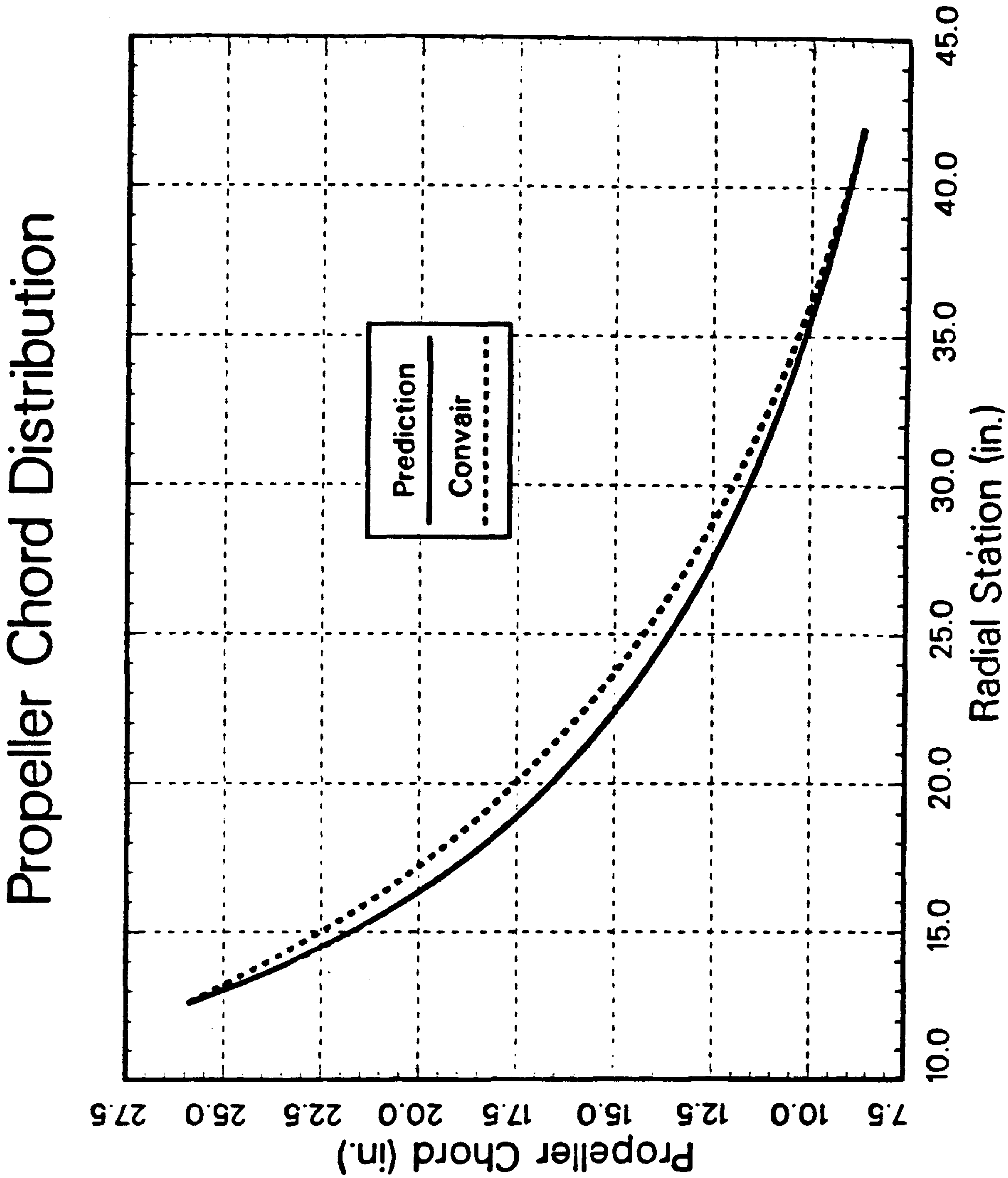

Figure 3: Verification of Propeller Chord Distribution

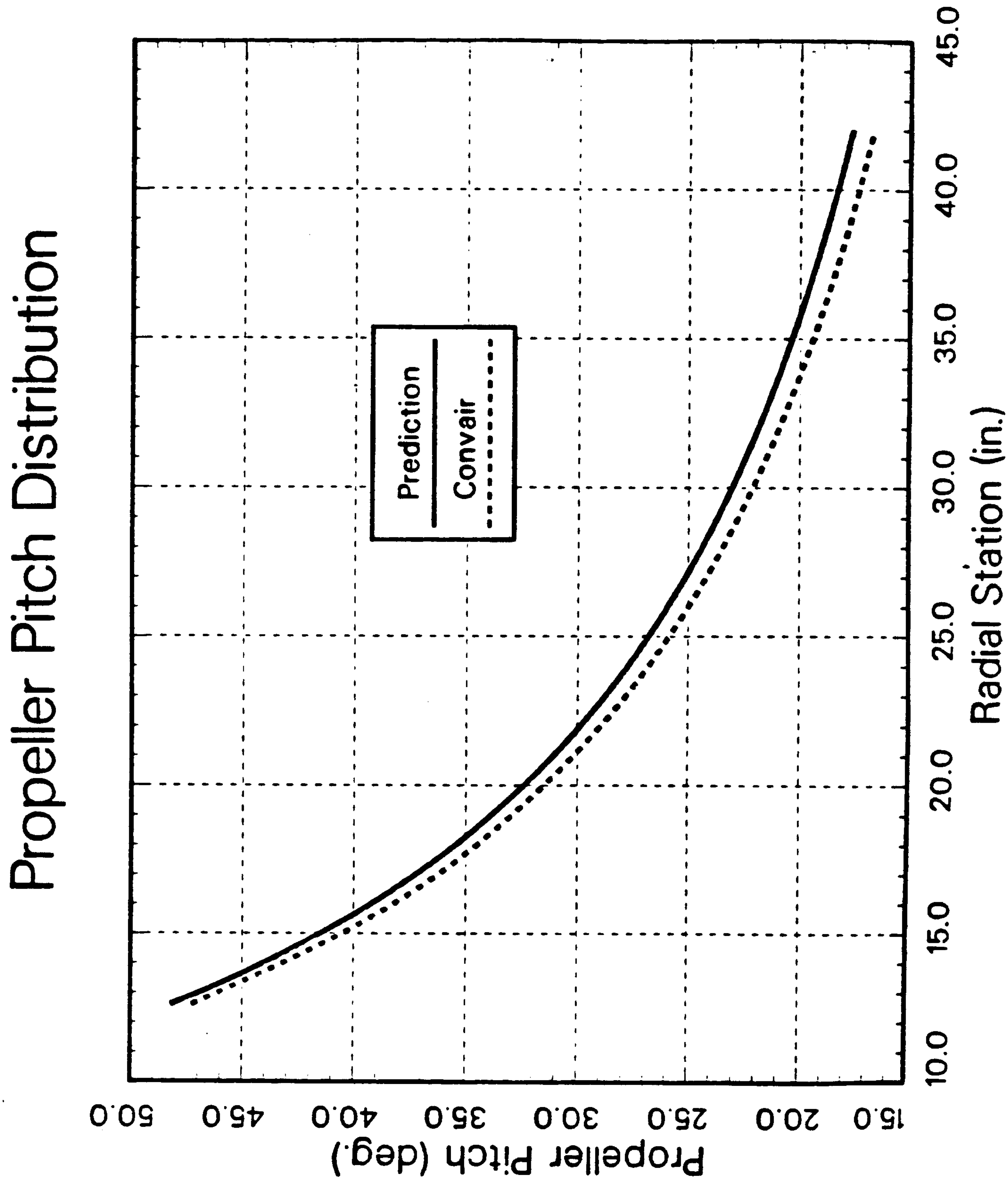

Figure 4: Verification of Propeller Pitch Distribution

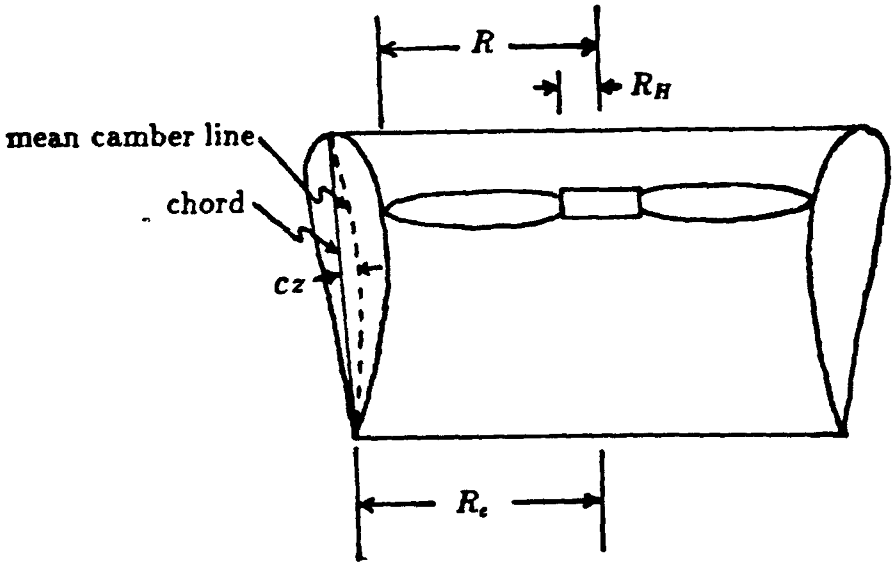

Figure 5: Ducted Propeller Geometry

4.3 Gõ 610 Blade

The second airfoil section whose thrust distribution is shown in Figure 6 is a circular arc airfoil; the Gõ 610. This airfoil section has a radius of curvature to chord ratio of 1.97. After losses are taken into account, the maximum L/D is 52.9 and the C_L has a value of 0.4248 at an angle of attack of 0.8°. The resulting blade which provides 85 lbs of thrust has a taper ratio of 1.52, a blade pitch angle of 32.78° at the root and 11.81° at the tip. The torque necessary to rotate the propeller at 7200 RPM is slightly higher, 10.40 ft-lbs. The power requirements for the same thrust are also slightly higher; 14.26 hp. This results in a slightly lower efficiency; 91.1%. The propeller geometry is shown in Figure 9 and the pitch distribution is shown in Figure 10. This airfoil, though it makes a larger and less efficient propeller, may be desirable because it is easier to manufacture.

4.4 Straightener Vanes

Both propellers use straightener vanes in the duct with NACA 0012 cross-sections and the vane pitch forced to 0°. The vane chords were restricted to be less than 13 inches to keep them completely in the duct. The vane pitch was restricted to 0° to embed structural members. These constraints resulted in 5 straightener vane blades in the duct to counter

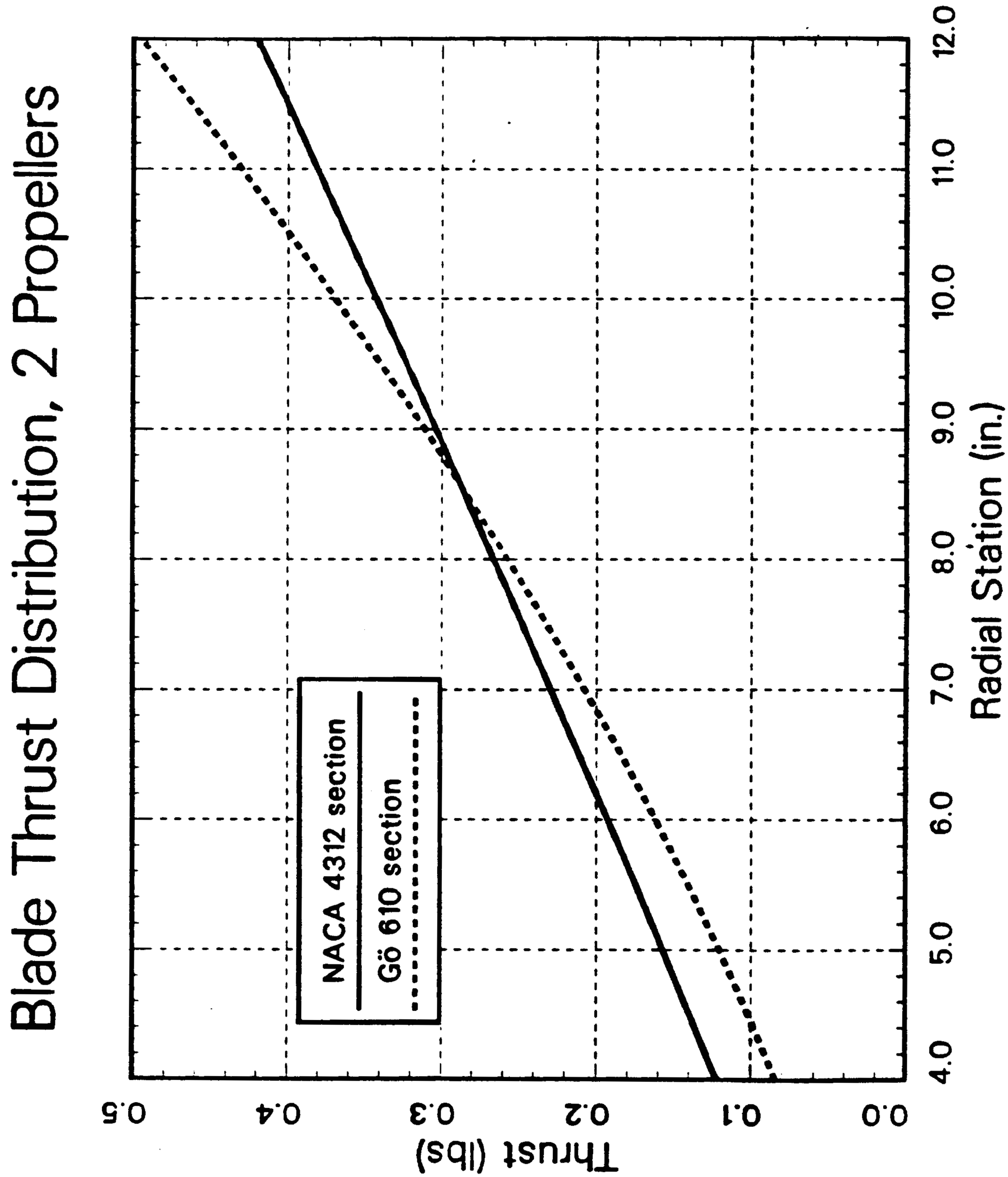

Figure 6: Thrust Distribution Comparison of Example Propellers

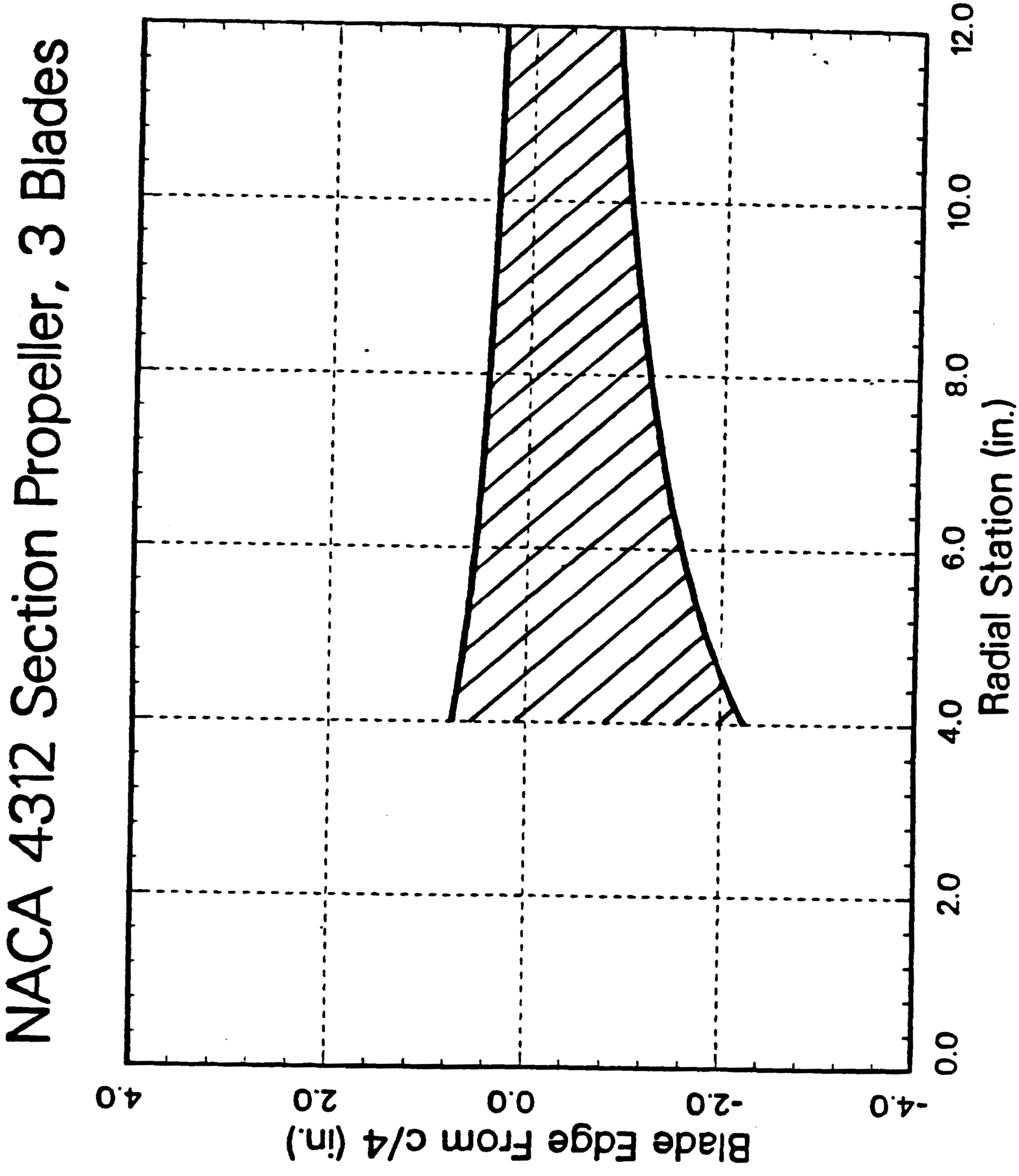

Figure 7: Example 1. Propeller Blade Untwisted Planform

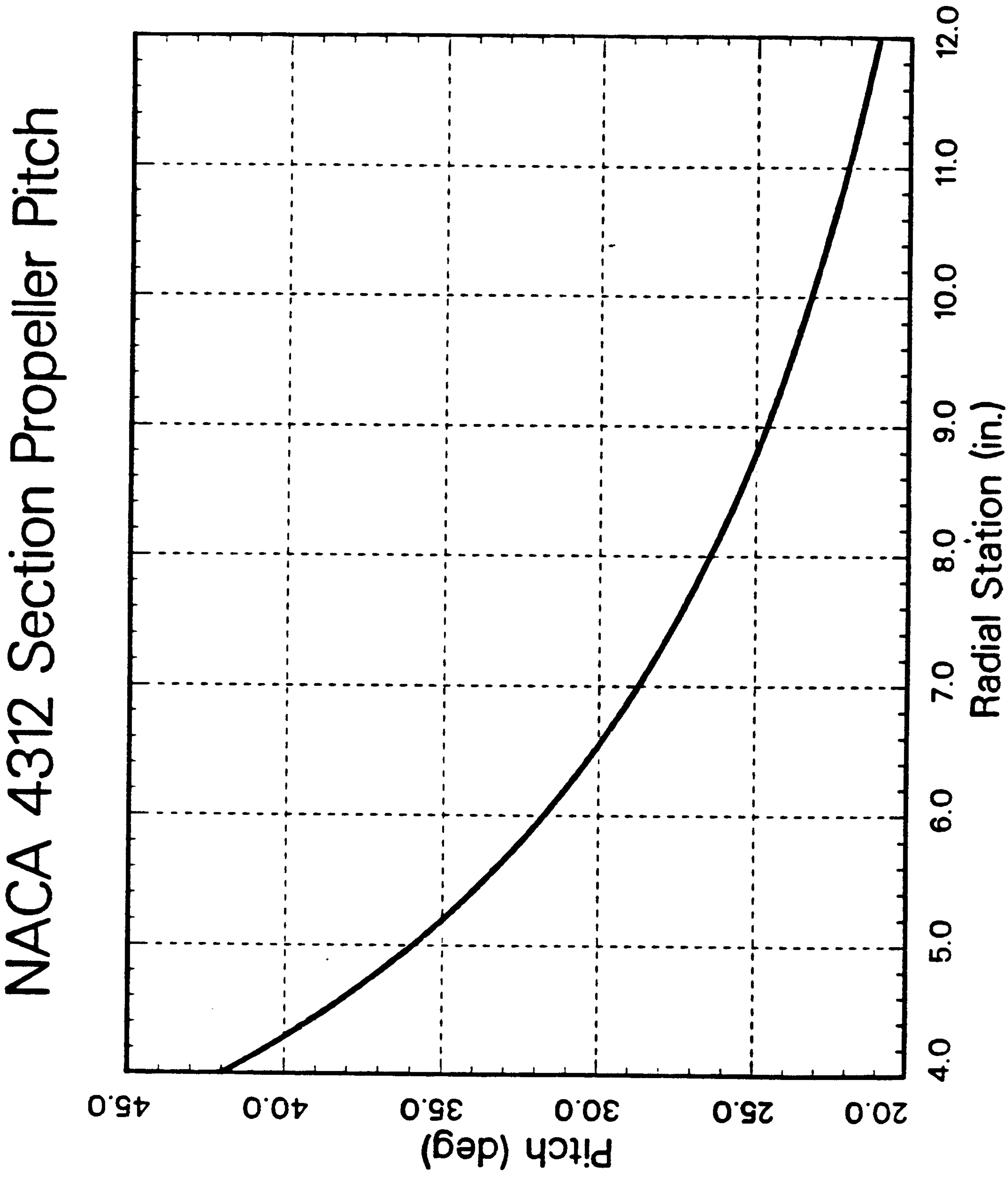

Figure 8: Example 1. Propeller Blade Twist Distribution

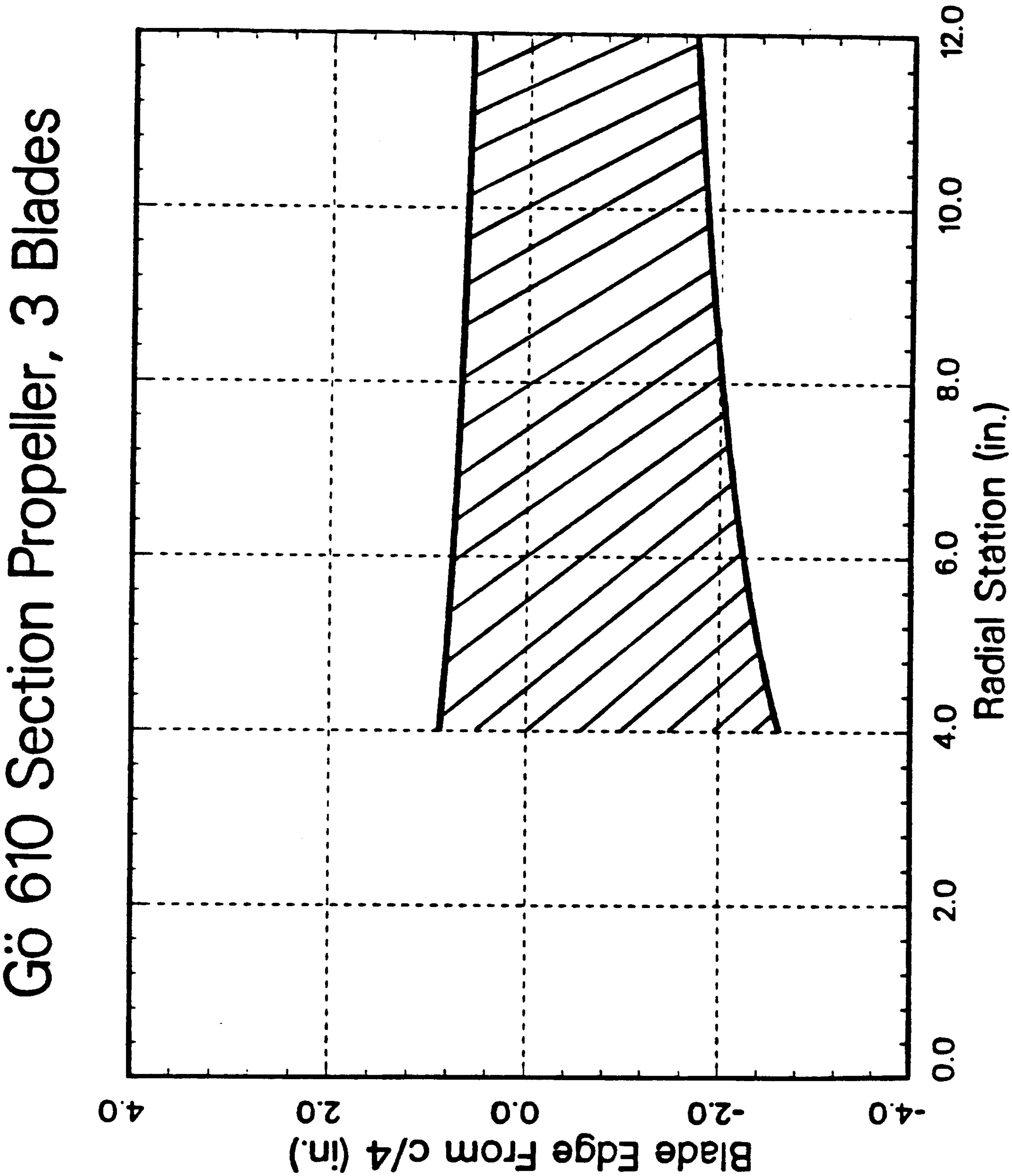

Figure 9: Example 2. Propeller Blade Untwisted Planform

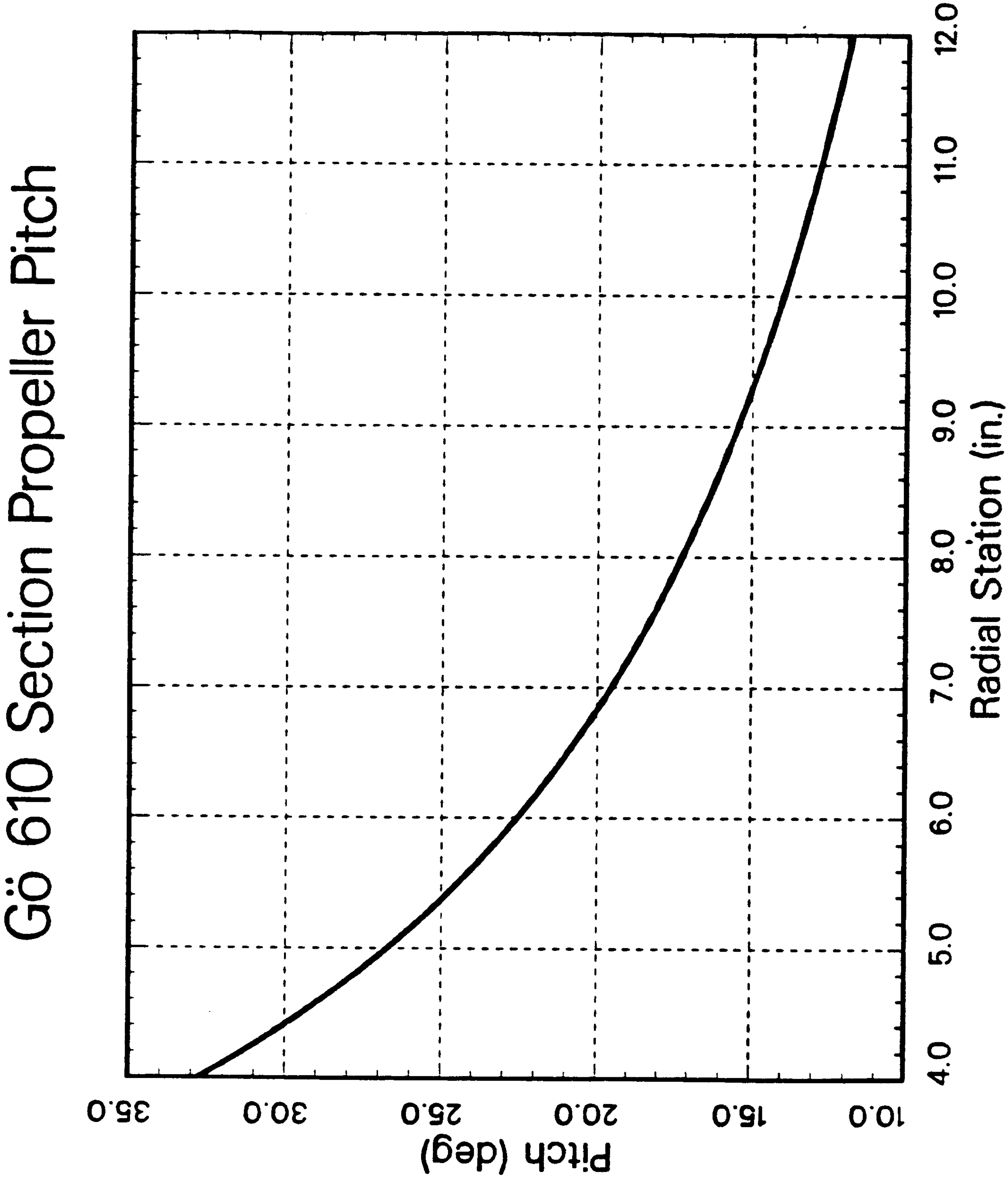

Figure 10: Example 2. Propeller Blade Twist Distribution

the propeller torque. The vane chord distributions resulting from both propellers are shown in Figure 11. It is interesting that the vane chord distribution curves are almost exactly the same as the thrust distribution curves on the propellers, but on a different scale. When the vane pitch is allowed to vary so as to maintain an L/D over the vane, the number of vanes is reduced to 4 and the similarity between the vane chord distribution and the blade thrust distribution breaks down. Figure 12 shows the vane chord distribution if the NACA 0012 is held at an L/D of 100 at an angle of attack of 10°. Letting the vane pitch angle vary, or changing the airfoil section has almost no effect on the resulting propeller, only on the size and number of the straightener vanes since the vanes provide only a very small part of the thrust.

5 Comparison to Experimental Results

5.1 Experimental Setup

To better understand the axial flow velocity at the propeller plane, an experiment was performed using a rake of 9 static pressure probes interspaced with 4 total pressure probes mounted downstream of the propeller. Ambient temperature and pressure readings were taken during the entire test so that air density values could be determined by the ideal gas equation. The velocities could then be determined through Bernoulli's equation.

The scope of the test included two propeller designs. Both of these designs were investigated at three rotational speeds both with the landing ring (which is 16 in. behind the duct exit) 6 ft above the ground and 1 in. above the ground. The rake of probes behind the propeller was moved to three locations for each of the conditions above. The two propellers that were investigated during the experiment were a composite blade using the chord distribution specified in the above Gō 610 airfoil section design and a wooden aircraft propeller cut to fit the duct. Both of these propellers were run at the maximum rotational speed the engine could produce (between 7590 RPM and 7740 RPM for the wooden propeller, and between 7110 RPM and 7350 RPM for the composite propeller). The wooden propeller was also run at 7000 RPM and 6250 RPM while the composite propeller was run at 6700 RPM and at 6000 RPM. This was to provide off-design data and to determine what factors were RPM sensitive.

5.2 Local Advance Ratio

The resulting data revealed two parameters which were insensitive to rotational speed; the local advance ratio, j, and the radial advance ratio, j'. The local advance ratio is the ratio of the inlet velocity at the propeller plane to the tangential velocity due to the propeller rotation at any blade span location; $j = \frac{V_A}{\Omega r}$. It is a function of the radial

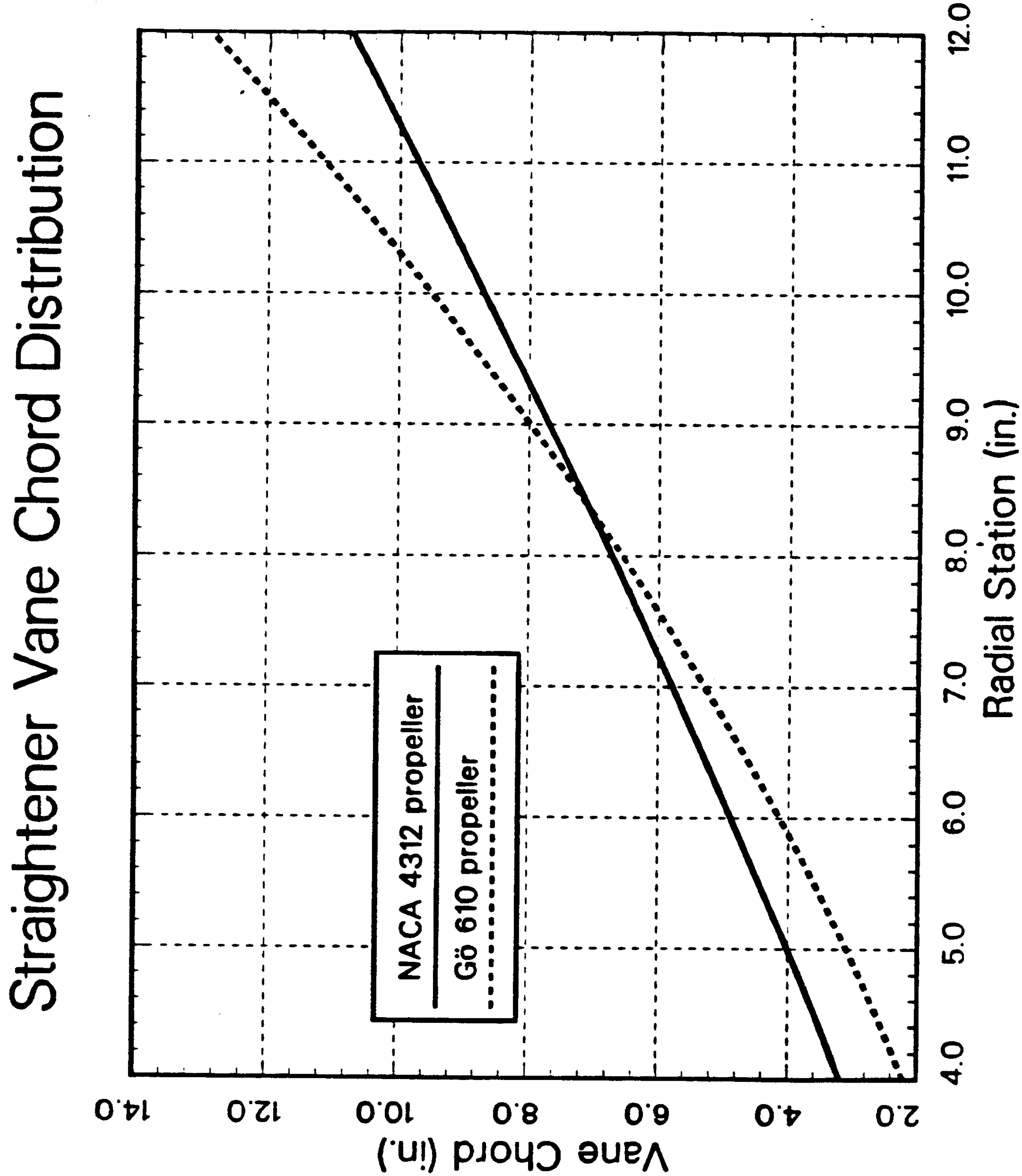

Figure 11: Straightener Vane Chord Distribution Comparison, No Twist

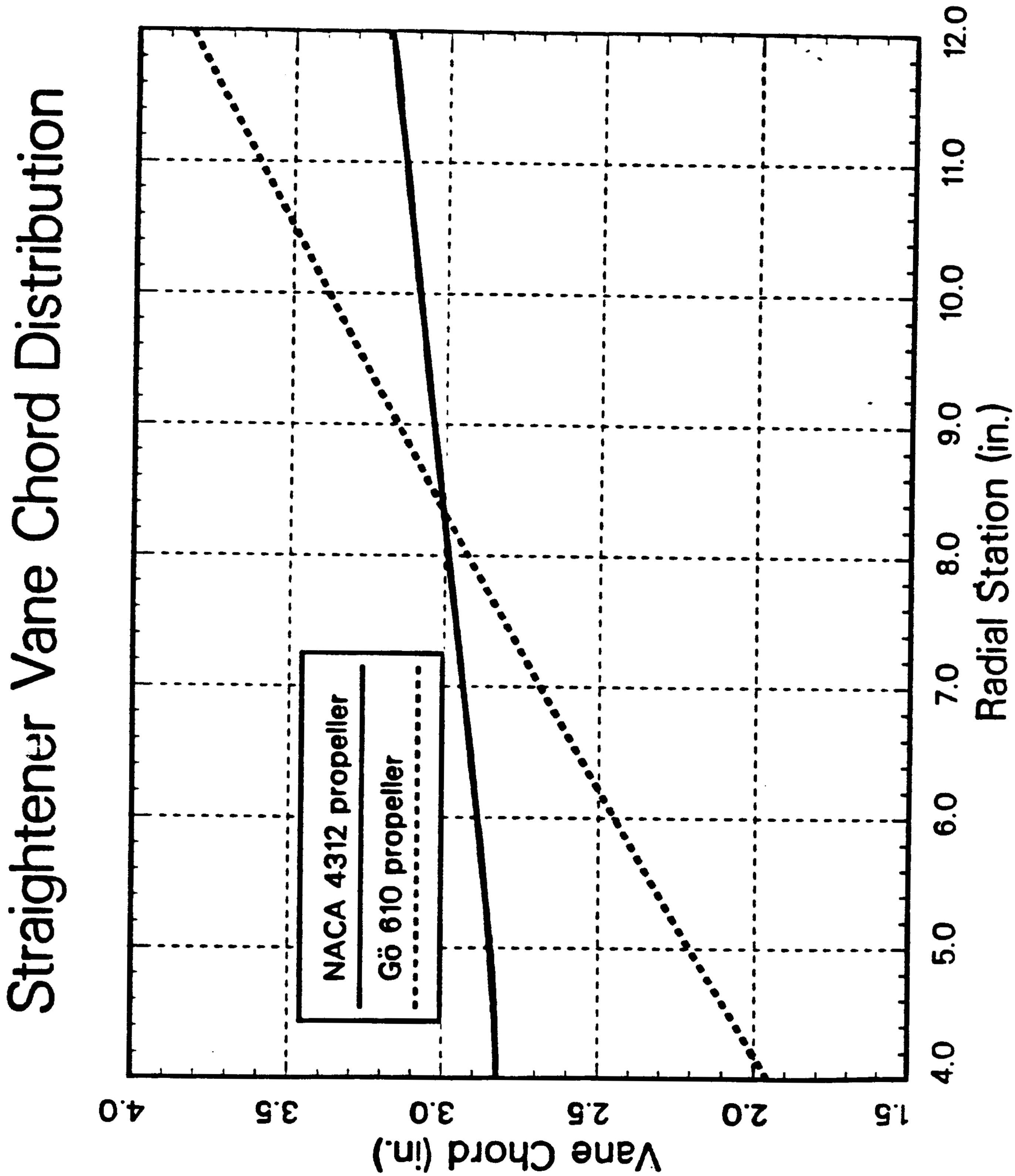

Figure 12: Straightener Vane Chord Distribution Comparison, Twisted

position only (see Figures 13-16). Max, Med, and Min RPM refer to the three rotational speeds mentioned above. Exact numbers are not quoted since constant speeds between runs couldn't be maintained, though variations were held within 2%. Figure 17 compares the experimental values of j distribution on the composite propeller to that predicted by the design analysis for the Gö 610 airfoil. The comparison is quite good, considering that the experimental propeller, though using circular arc airfoils, used a varying radius of curvature to chord ratio along the span, which changed the sectional characteristics from the design. The pitch distribution also differed from the design values. A severe loss in induced velocity is apparent near the tip of the blade, apparently due to pressure leakage around the tip through the gap between the tip and the duct wall, or due to interaction between the duct wall boundary layer and the blade tip.

Another aspect shown in Figure 17 is that the local advance ratio should theoretically be a function of RPM. The assumptions used in the off-design analysis are possibly not valid since the resulting thrusts and mass flow rates are matched to the desired RPM. This is not done through calculating the flow resulting from the desired RPM and resulting thrust, but from the lift off of the propeller. That lift is then used to determine the total thrust which determines the mass flow rate. A more accurate, but time consuming method would be to determine the mass flow due to the RPM and then the thrust. The lack of dependence on RPM of the experimental values of j could be due to the blade untwisting when the RPM increases, so that the sectional angles of attack and their C_l's increase which induces more axial flow. This could maintain approximately the same local advance ratio at any RPM. The mechanism causing this untwisting could be centrifugal force, or the aerodynamic pitching moments of the blade sections. The fact that the analysis assumes a constant blade cross-sectional shape while the actual propeller cross-section changes along the span may also explain the independence of RPM. If some sections are stalled, or at negative angle of attack, at one RPM, but are not at other RPM, the characteristics of the propeller would alter for the other RPM. This dependence on the RPM of the local advance ratio in the theoretical results suggests that the theory will not adequately predict off-design performance; as the RPM change further from the design value, the local advance ratios will be increasingly inaccurate.

Figure 18 compares the local advance ratios of both propellers at maximum rotational speed 6 ft above and 1 in. above the ground. This figure indicates that there is very little ground effect on the composite propeller the ground effect is more pronounced on the wooden propeller. Tip effects are also alleviated on the composite propeller while they are enhanced on the wooden propeller in the presence of the ground. Why this is is unclear, especially considering that the thrust of the wooden and composite propellers either remains the same or decreases in the presence of the ground. The most marked difference occurs near the hub of the wooden propeller so the ground effect may disturb the flow at the hub to blade transition more. The wooden propeller's length of transition from hub to blade is longer than that of the composite propeller.

The effect on the tip losses of the two blades when in the ground effect region are

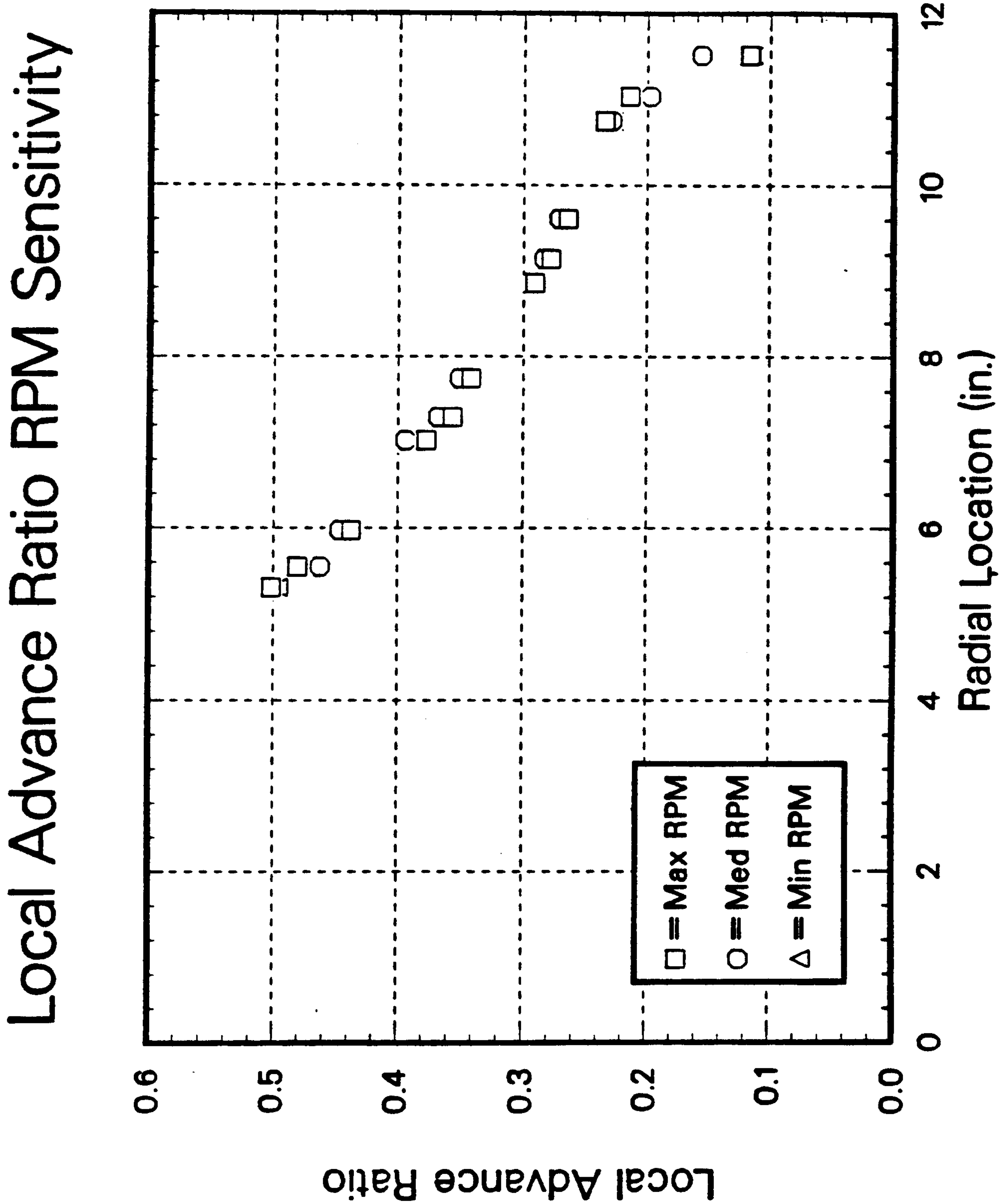

Figure 13: Composite Propeller j Distribution 6′ Above Ground

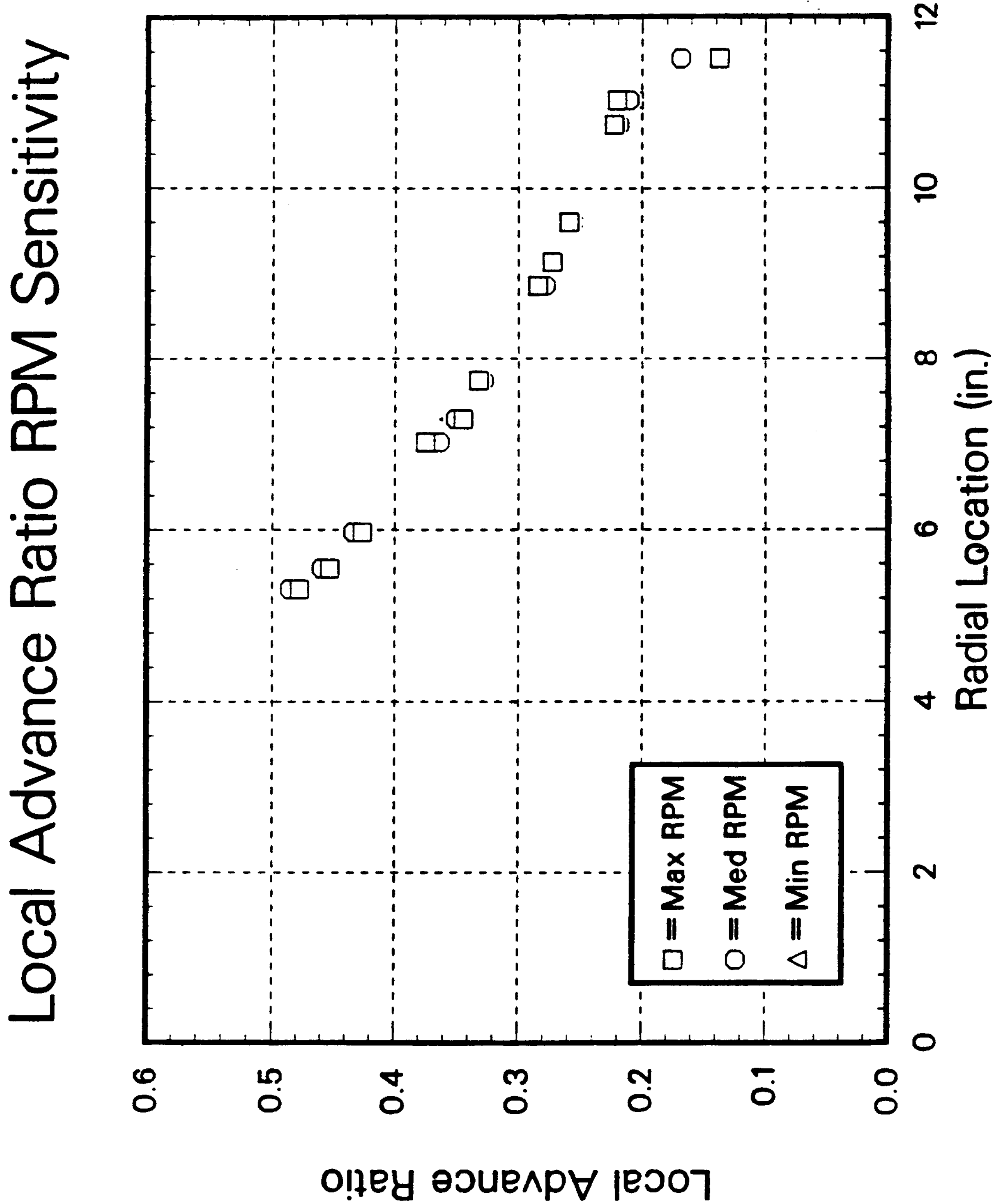

Figure 14: Composite Propeller j Distribution 1″ Above Ground

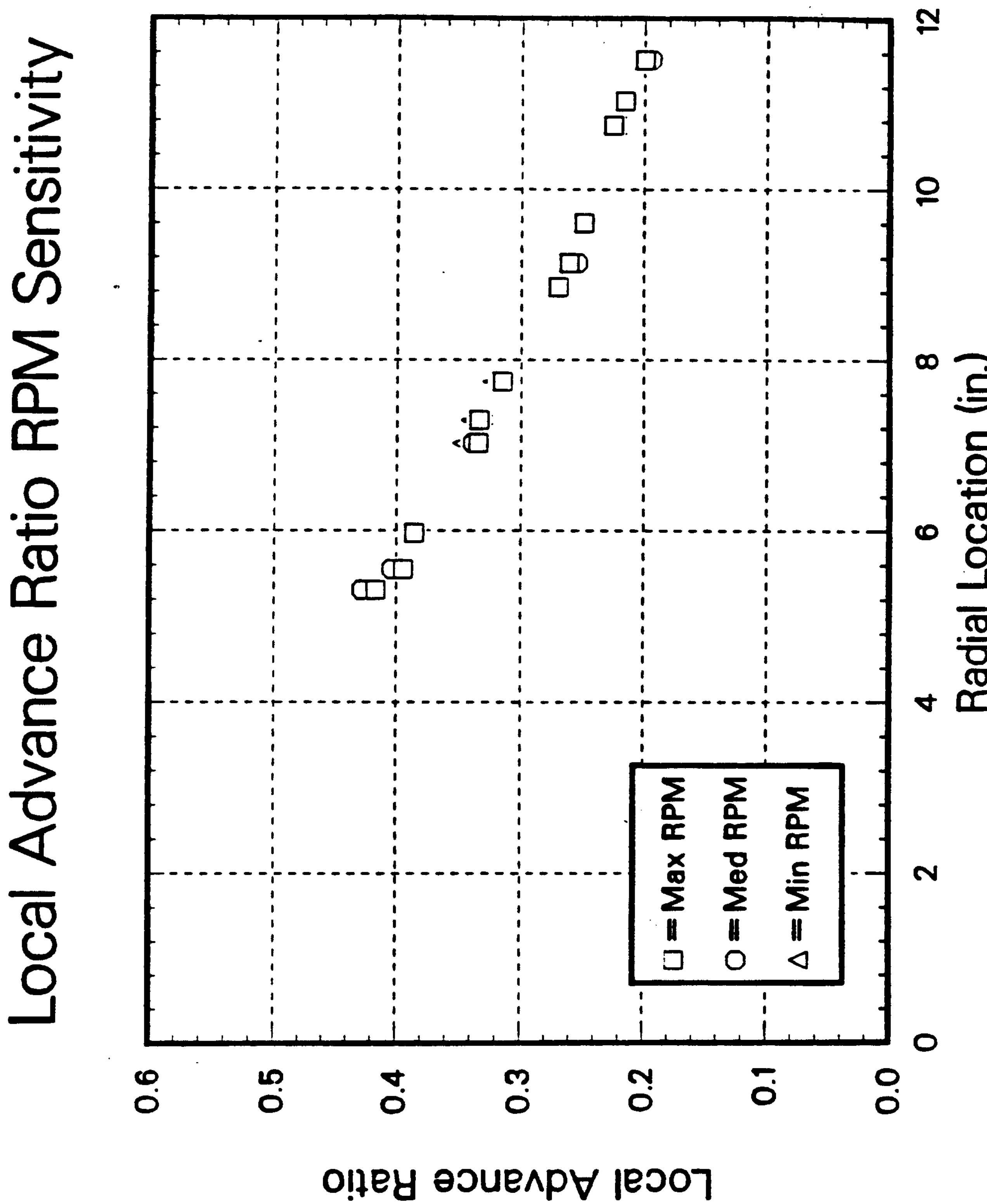

Figure 15: Wooden Propeller j Distribution 6′ Above Ground

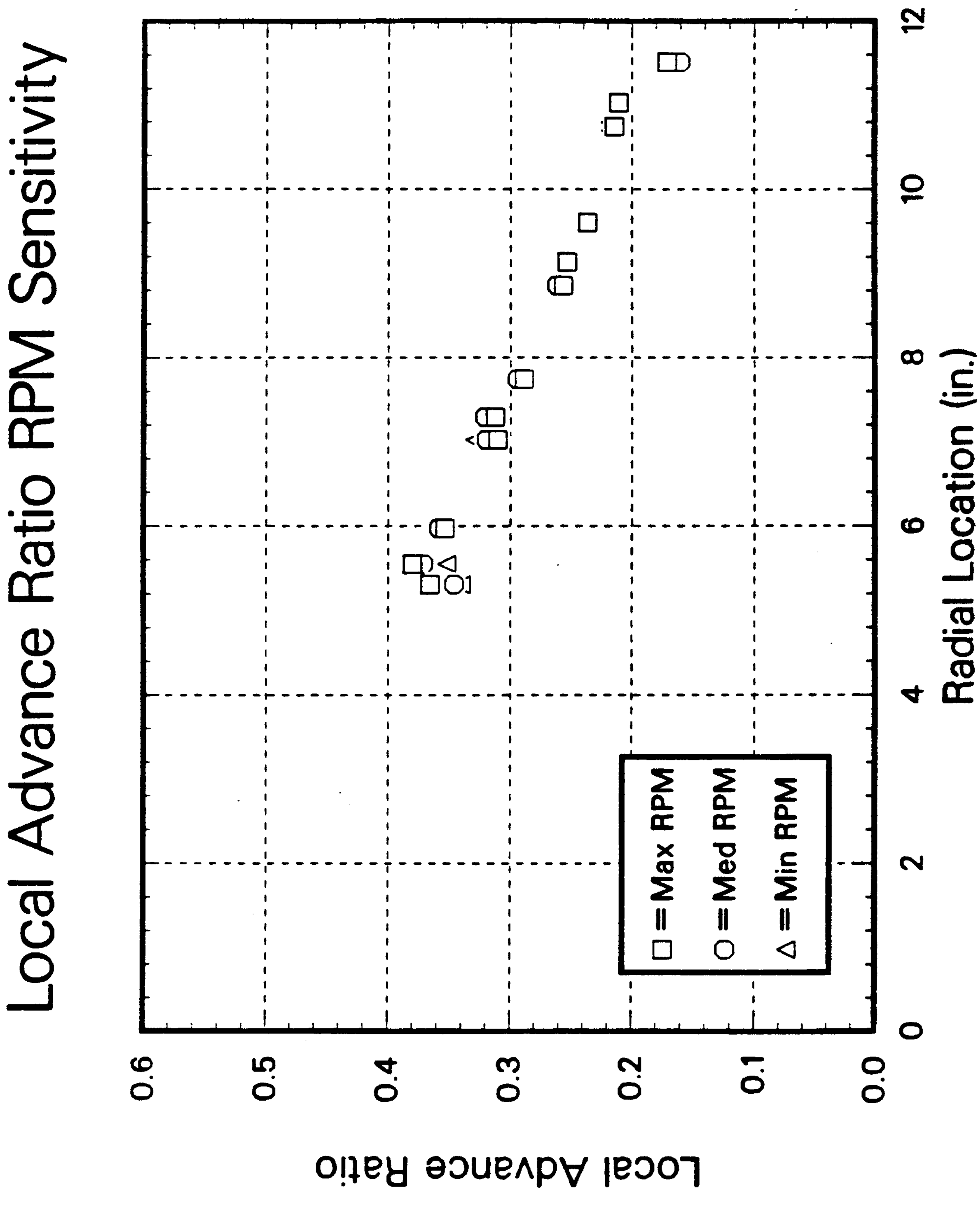

Figure 16: Wooden Propeller j Distribution 1″ Above Ground

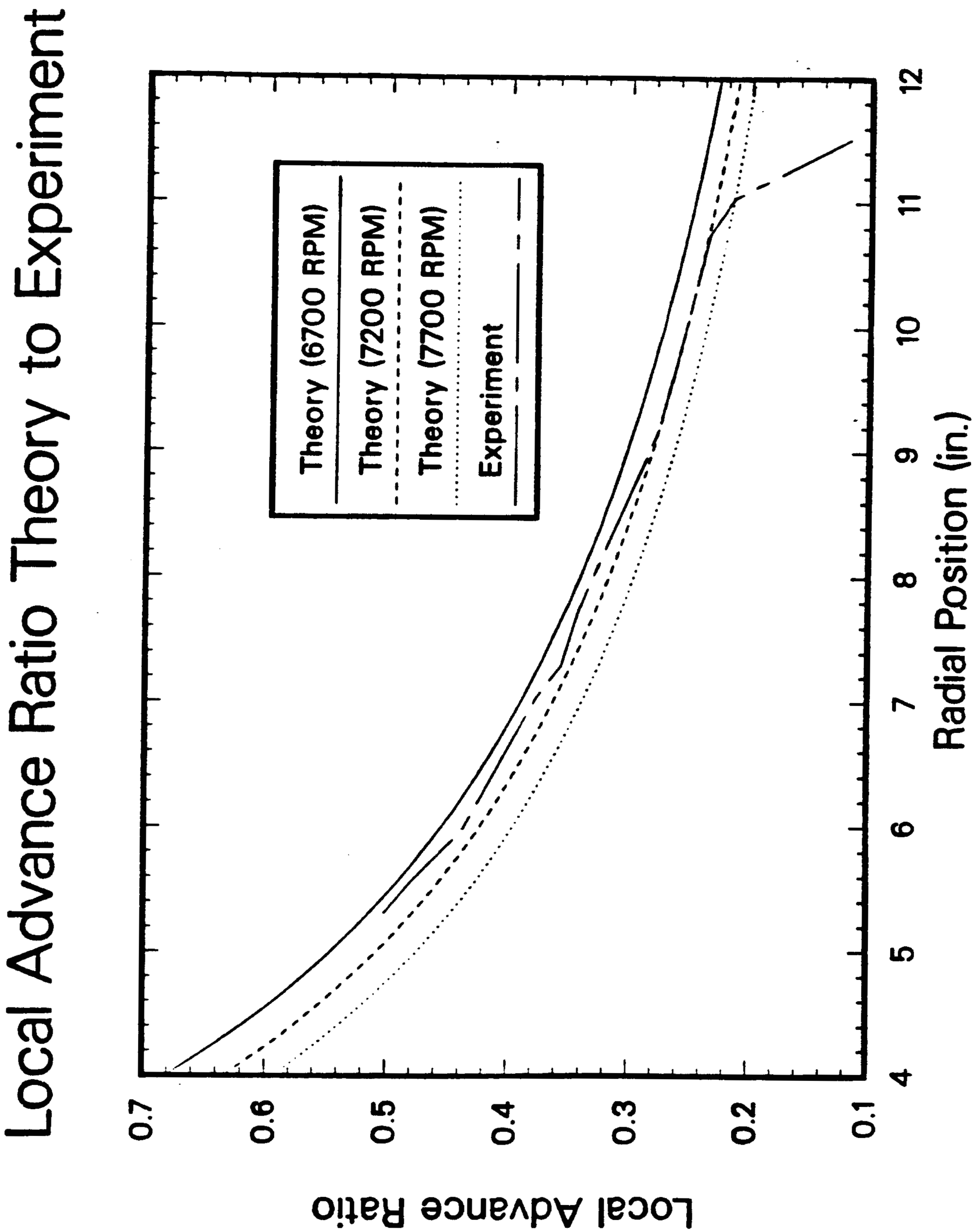

Figure 17: Composite Propeller j Distribution Comparison

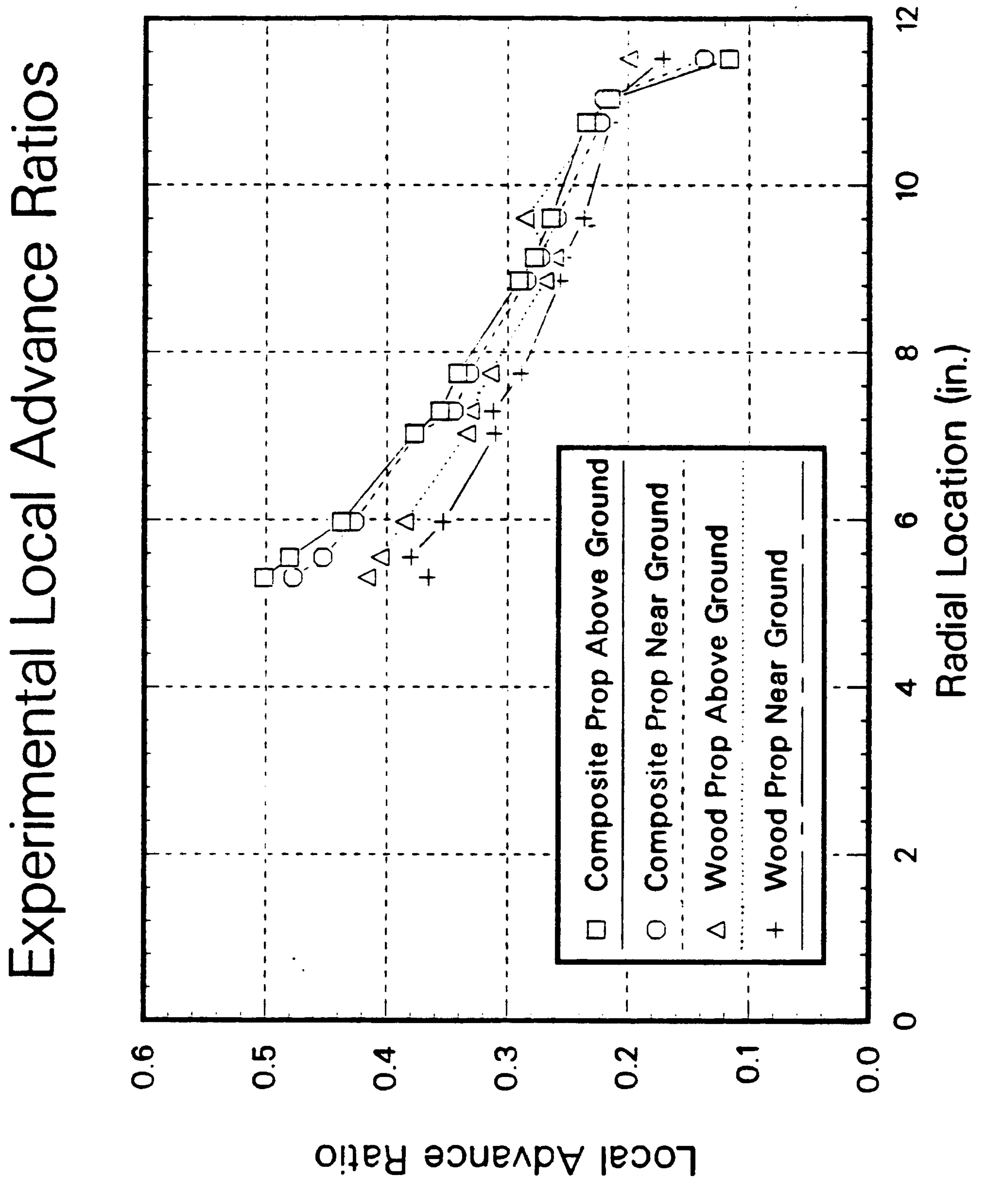

Figure 18: Ground Effect on j Distribution

also unclear. The losses of the composite blade are more pronounced than those of the wooden blade, but the ground effect seems to be beneficial to the composite blade while being detrimental to the wooden blade. The major difference between the two propellers at the tip is that the chord of the wooden propeller is larger than that of the composite blade. Since the ground effect inducement of greater tip losses on the wooden propeller still doesn't produce tip losses of the magnitude of the composite propeller tip losses in ground effect, a high tip chord to tip gap ratio would be desirable. This appears to be the only clear position that is derivable from the data though.

5.3 Radial Advance Ratio

If the local advance ratio is multiplied by the square of the fraction of the blade span at each location, $\left(\frac{r}{R}\right)^2$, another nondimensional parameter is produced, $j' = \frac{Vr}{\omega R^2}$, which may be called the radial advance ratio since it is dependent on the fraction of the radius at which it is calculated. Figures 19-22 show an interesting correlation. Like the local advance ratio, the radial advance ratio is not a function of the RPM of the propeller, but of radial location only. The noteworthy aspect of this parameter is that it is linear with radial location, up to the region where tip effects occur. The sensitivity of this parameter to tip effects appears to be more dramatic than the sensitivity of the local advance ratio. Figure 23 shows about the same sensitivity to ground proximity as the local advance ratio has; that the ground proximity appears to lessen tip effects on the composite blade, while enhancing tip spillage with the wooden propeller.

5.4 Thrust Coefficient

Figures 24 and 25 directly show the effect of RPM and the ground proximity on thrust. Though a high degree of scatter is present, the thrust coefficient, based on propeller tip speed ($V_T = \Omega R$), $C_T = \frac{T}{\frac{1}{2}\rho V_T^2 A}$, tends to increase when the ground is near and decrease slightly with RPM. The thrust coefficient data associated with the composite propeller is more highly scattered than that associated with the wooden propeller. This could be due to a number of causes: the leading edge of the circular arc airfoil is much sharper, making it more susceptible to stall than the wooden blade, the method of measuring the thrust (reading an LED scale against a bright sky background), and the composite blade producing more thrust which increases the disk loading making it more susceptible to stall.

Figure 26 shows, again, how the theoretical analysis on the propeller becomes less and less accurate away from the design RPM of 7200. This is most likely due to the differences in blade section and twist from that of the proposed design and the possibility of blade untwisting under load. An improvement in the analysis would be to include the blade material properties so that untwisting could be modeled.

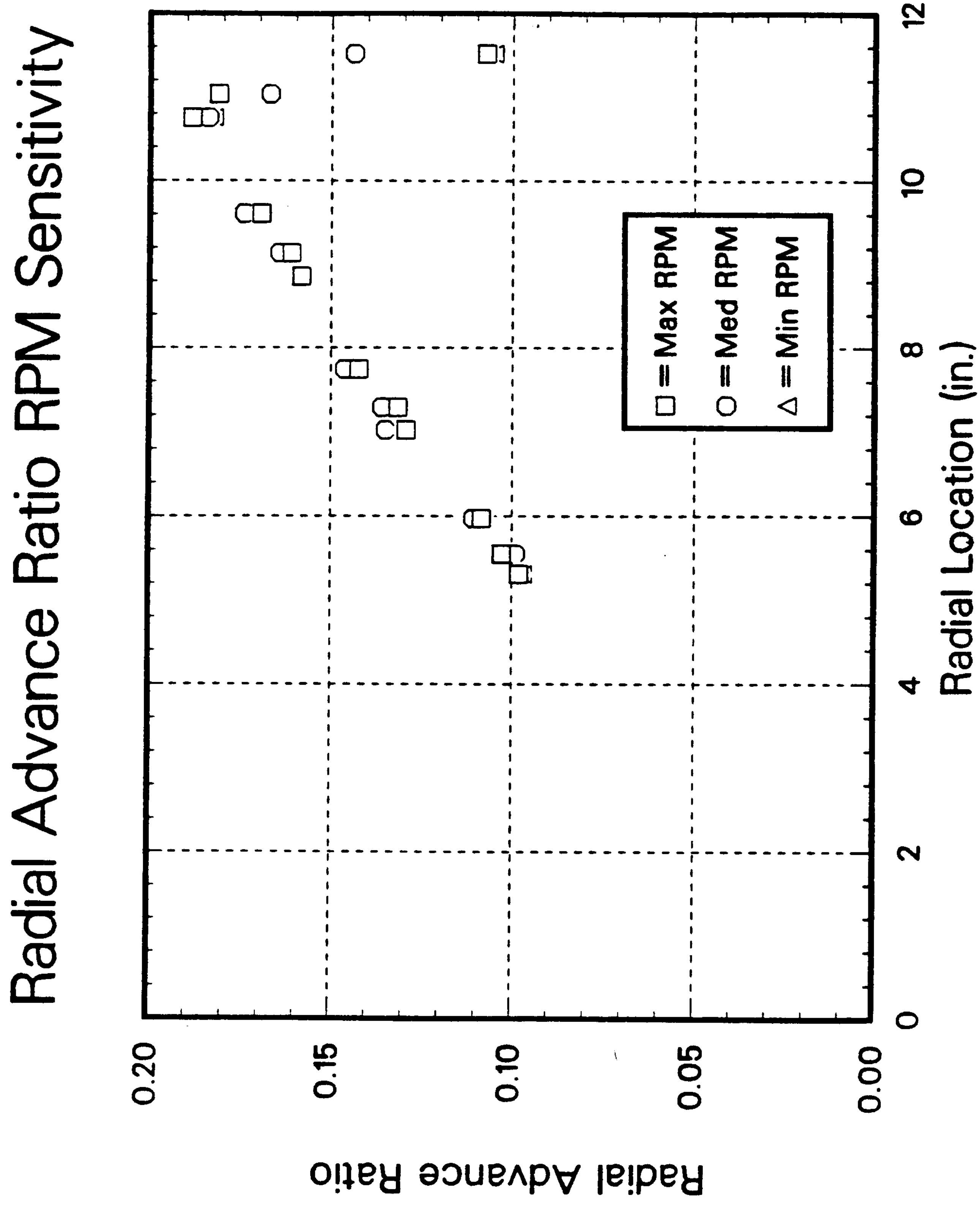

Figure 19: Composite Propeller j' Distribution 6′ Above Ground

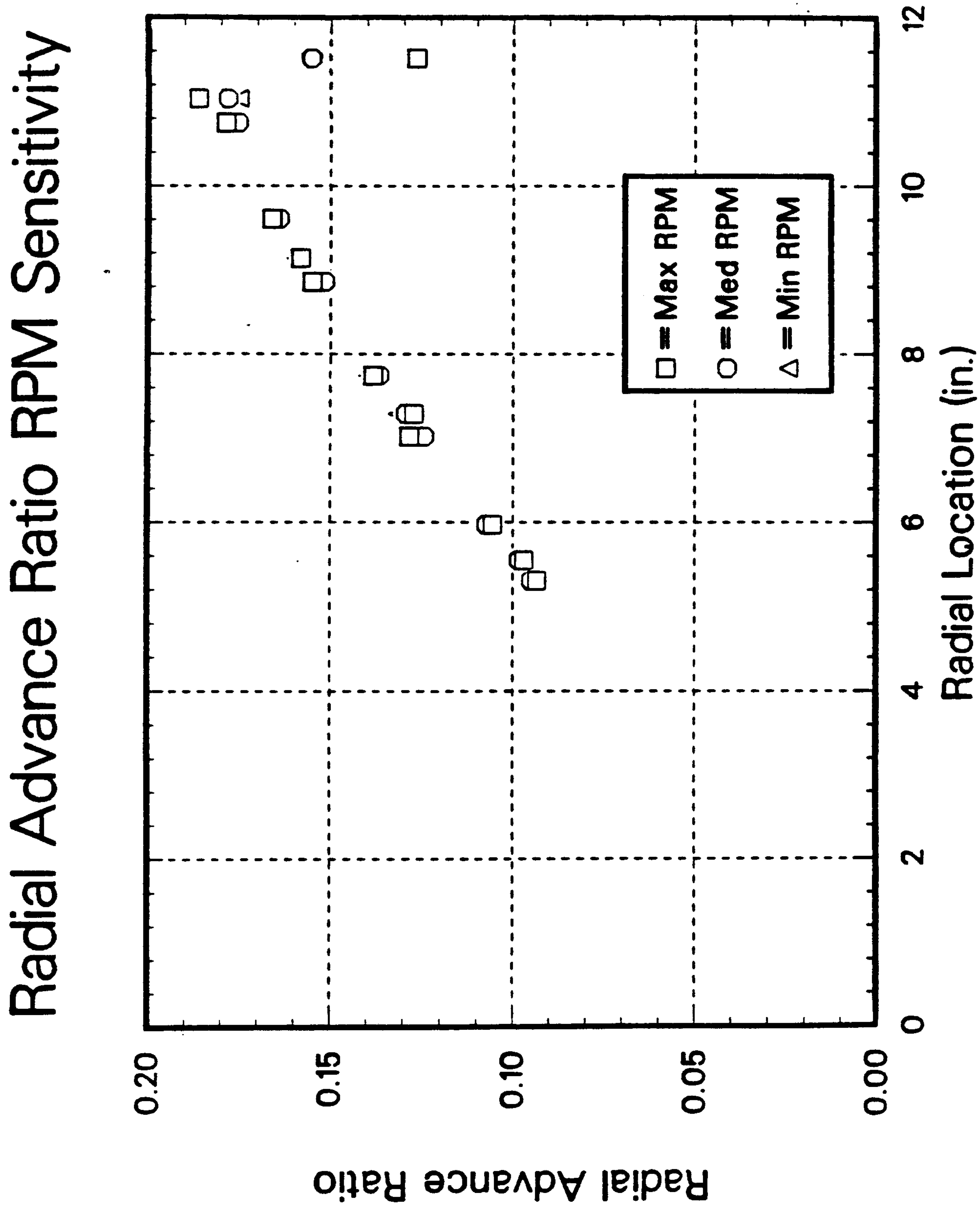

Figure 20: Composite Propeller j' Distribution 1″ Above Ground

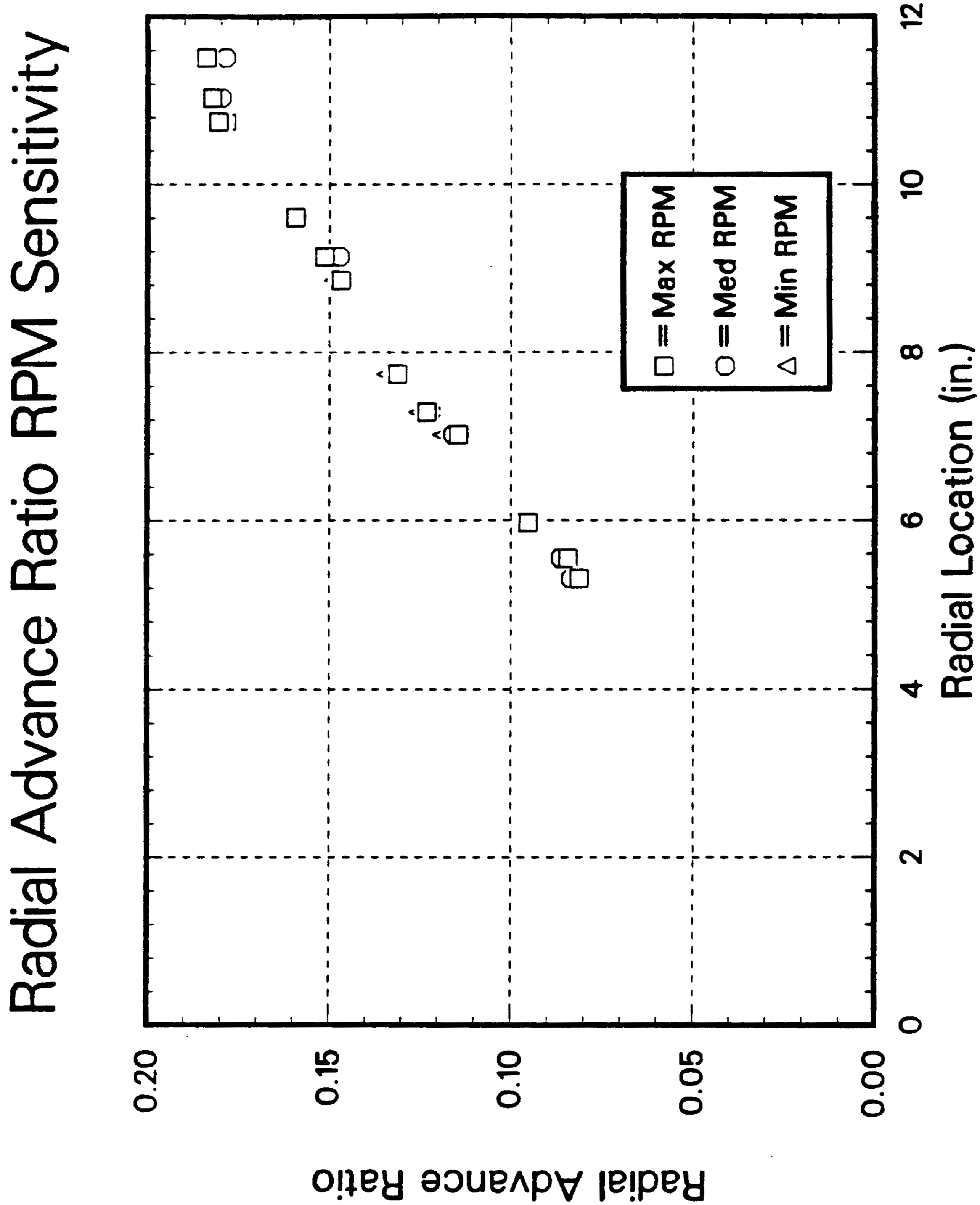

Figure 21: Wooden Propeller j' Distribution 6′ Above Ground

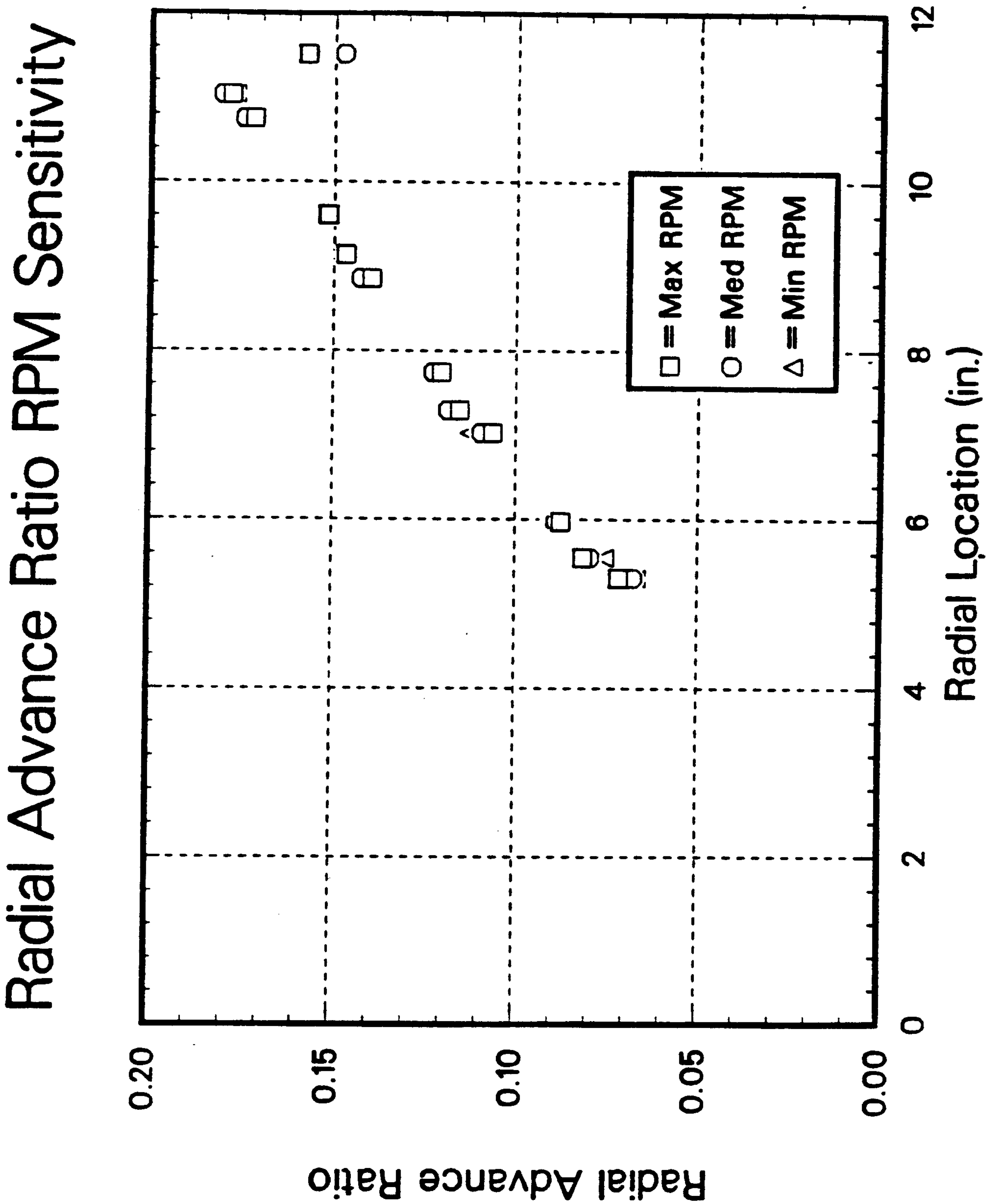

Figure 22: Wooden Propeller j' Distribution 1″ Above Ground

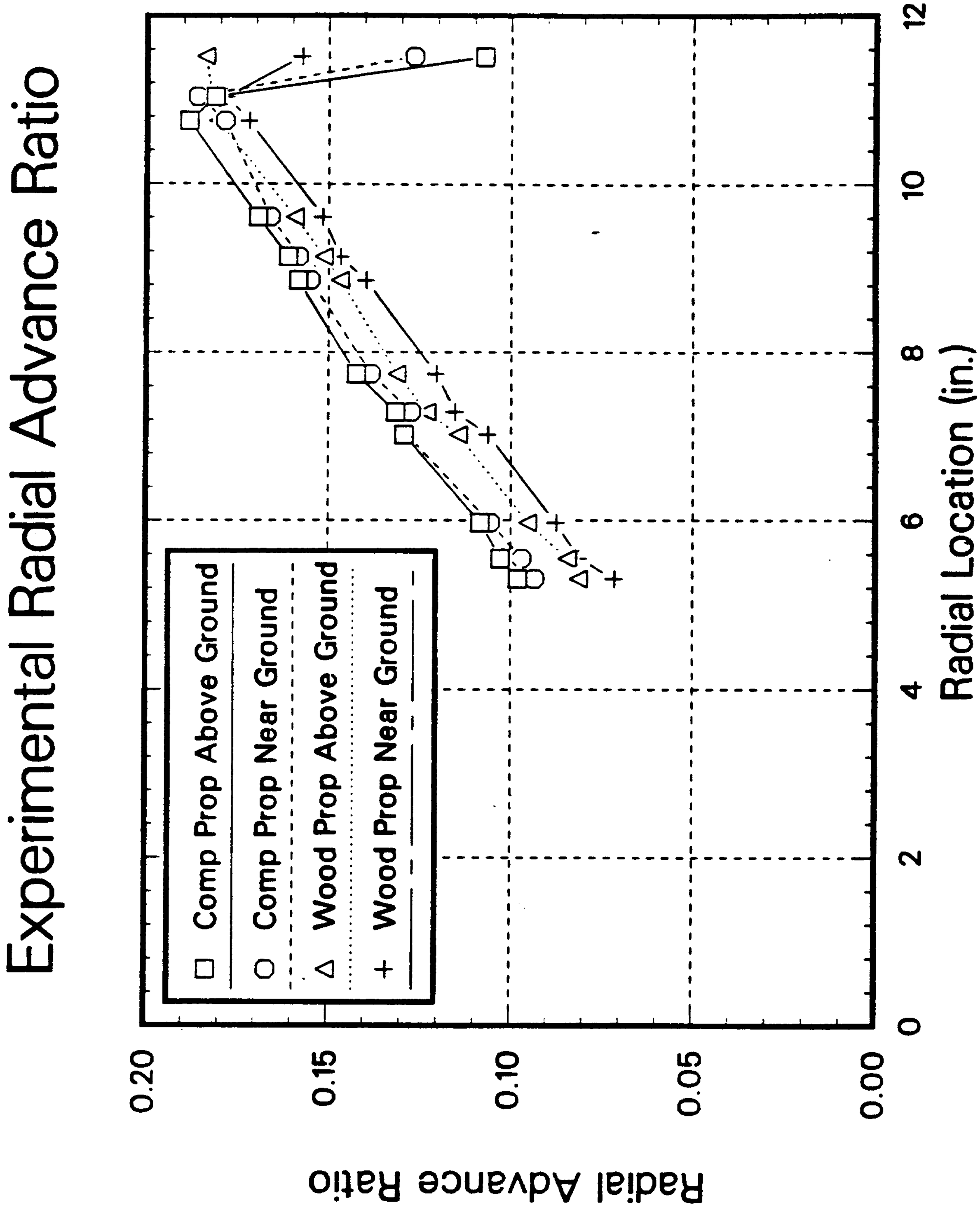

Figure 23: Ground Effect on j' Distribution

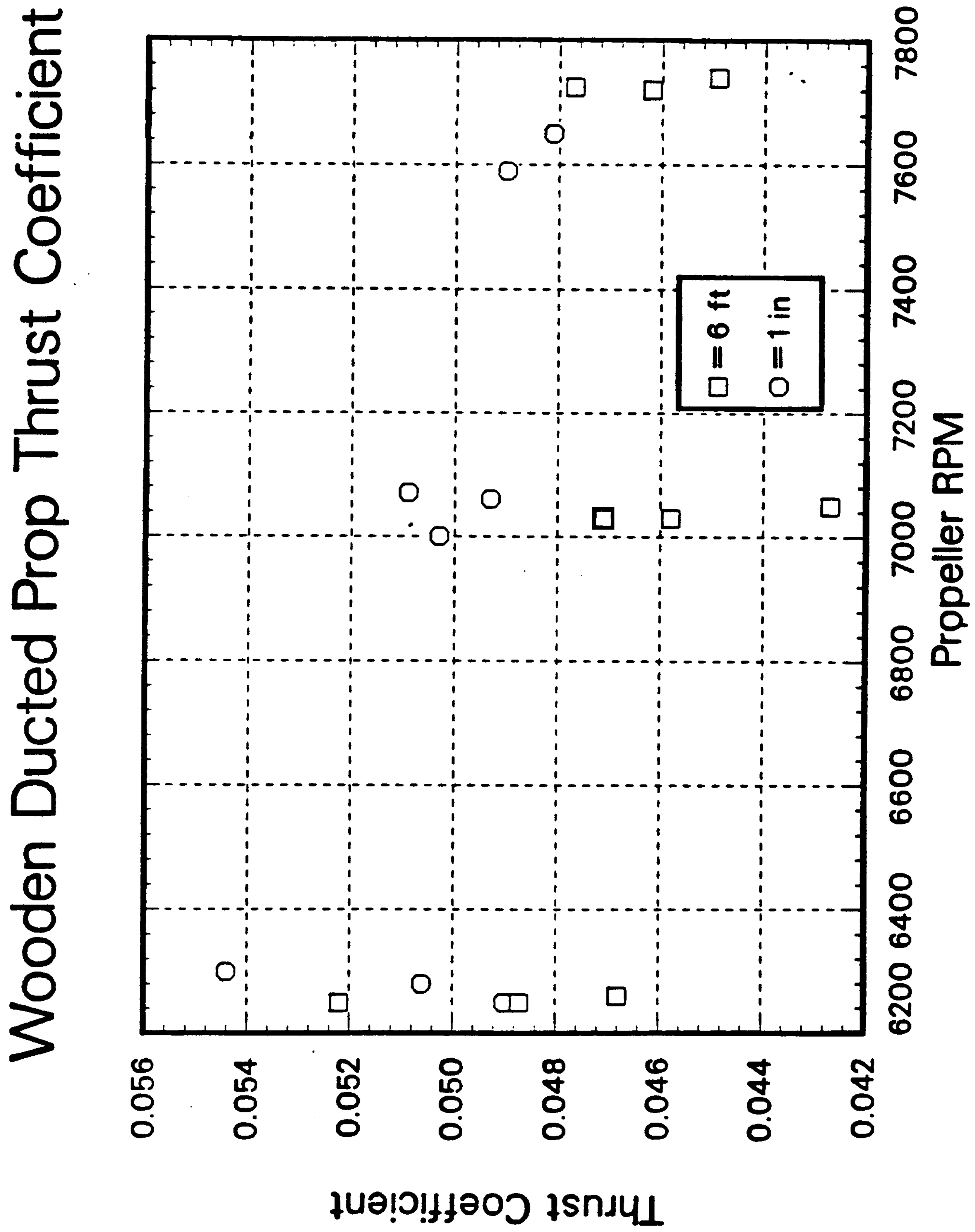

Figure 24: Wooden Propeller C_T RPM and Ground Sensitivity

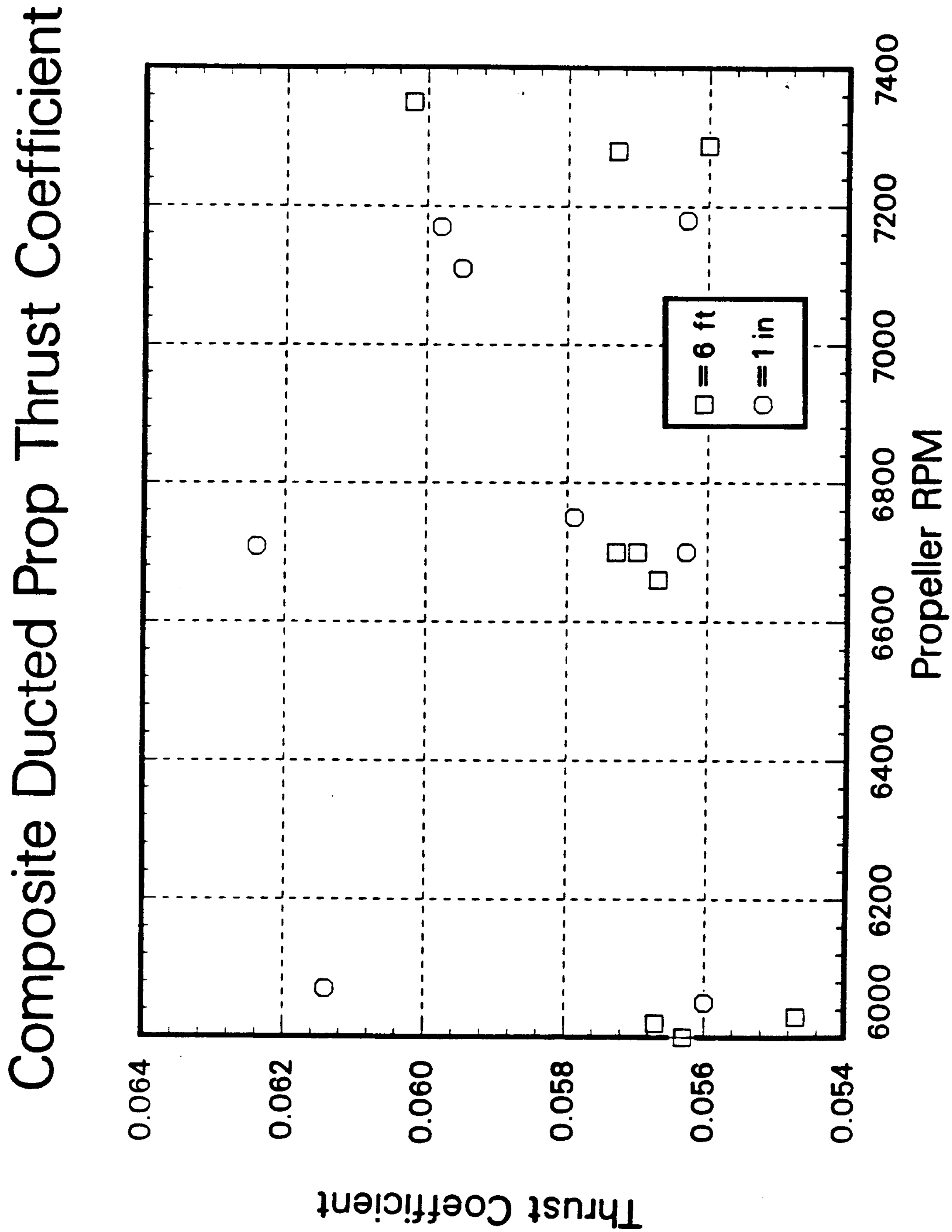

Figure 25: Composite Propeller C_T RPM and Ground Sensitivity

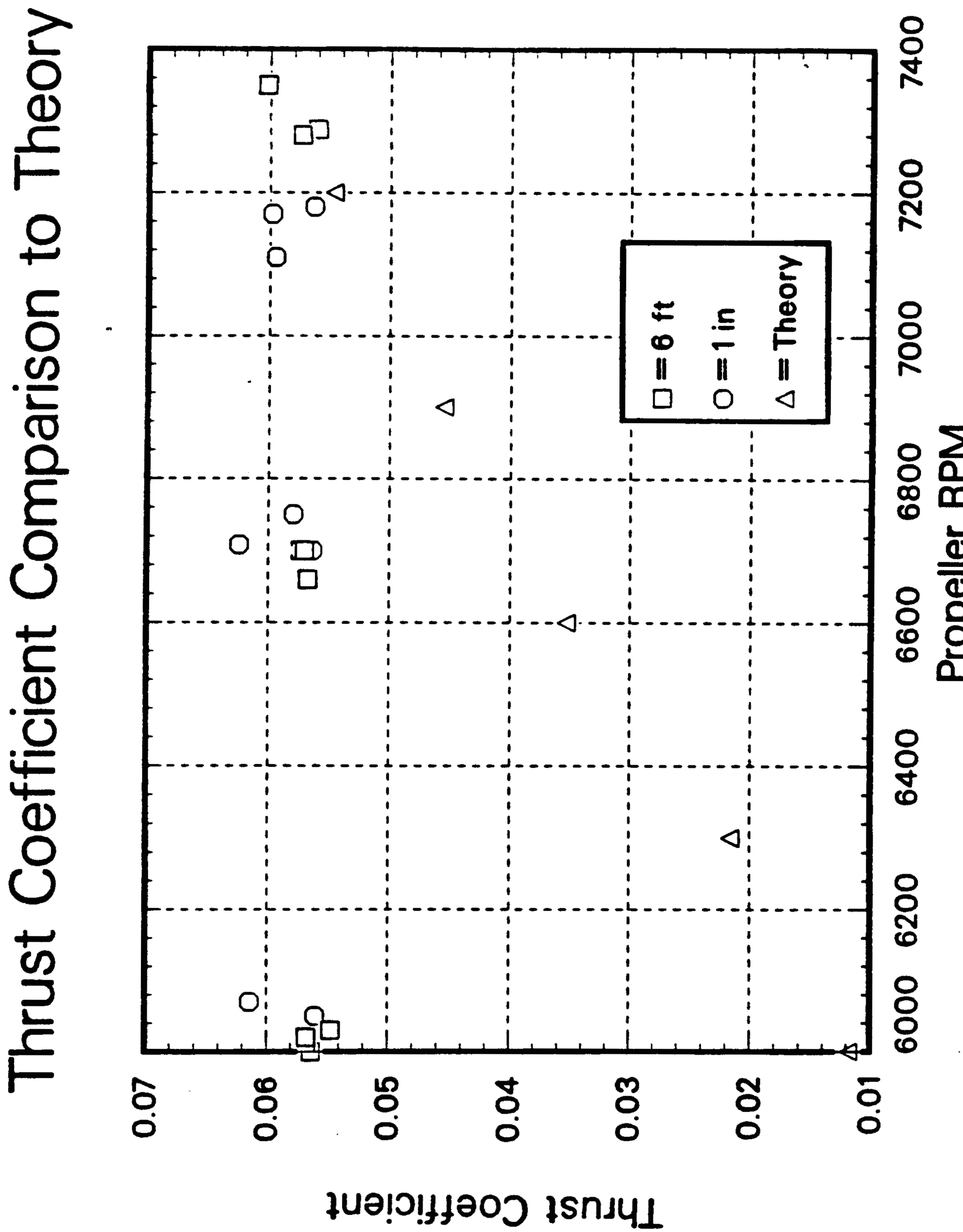

Figure 26: Composite Propeller C_T Comparison To Theory

6 Conclusions

The design of a propeller blade for a ducted propeller can be very complicated. However, using several simplifying assumptions, a fairly accurate prediction of performance for a blade designed for operation under specific conditions can be made. The reduction in complexity reduces the computation time by much more than the reduction in accuracy. No more than 6% error is seen in the design comparable to the Convair propeller design, while no potential equations need to be solved.

Using this analysis to determine off-design performance is not as accurate, though. In fact, reducing the RPM of the blade 600 RPM from the design speed results in a 40% error in the thrust coefficient. So, while the analysis is fairly accurate in designing a propeller blade and set of straightener vanes to yield required performance at specific design conditions, it is not trustworthy for predicting off-design performance.

The reason for the inaccuracies may lie mainly in structural considerations. Flexing and twisting of the blade away from its original shape cause changes in the operating conditions not considered in the analysis. A possible improvement would be the inclusion of the sectional pitching moment and blade material properties. It is also probable that the differences in the tested blade geometry from that of the blade in the analysis could account for the differences in off-design performance. Another possibility is inaccurate assumptions in the off-design RPM analysis. Or, it could be a result of a combination of the above. These drawbacks do not outweigh the speed and accuracy of the analysis at the design condition, however.

References

1. Sheehy, T. W. , "Computer Aided Shrouded Propeller Design", AIAA Paper No. 73-54, 1973.

2. McCormick, T. W. , Jr. , Aerodynamics of V/STOL Flight , Academic Press, New York, N. Y. , 1967.

3. Helmbold, H. B. , "Range of Application of Shrouded Propellers", Engineering Report No. 189, University of Wichita, Wichita, KS, 1955.

4. Lazareff, M. , "Aerodynamics of Shrouded Propellers", AGARDograph 126, Paper D, pp 237-289.

5. Kucheman and Weber, Aerodynamics of Propulsion , McGraw Hill Book Company, Inc. , New York, N. Y. , 1953.

6. Pope, Alan, and Harper, Low Speed Wind Tunnel Testing , Wiley and Sons, New York, N. Y. , 1966.

7. "Proposal For AID, Vol. I, Technical Proposal", GDC PIN 66-947, Nov. , 1966, pp 4-8–4-46.

8. Jacobs, E. N. , Ward, K. E. , and Pinkerton, R. M. , "The Characteristics of 78 Related Airfoils Sections From Tests in The Variable-Density Wind Tunnel", NACA TR-460.

9. Lindsey, D. , Stevenson, D. B. , and Daley, B. N. , "Aerodynamic Characteristics of 24 NACA 16-Series Airfoil Sections at Mach Numbers Between 0.3 and 0.8", NACA TN-1546, 1948.

10. Riegels, F. W. , Aerofoil Sections: Results From Wind-Tunnel Investigations Theoretical Foundations , Butterworths, London, 1961.

11. Abbott, I. H. , and Von Doenhoff, A. E. , Theory of Wing Sections, Dover Publications, Inc, New York, N .Y . , 1959.

Appendices

A Ducted Propeller Design Code

```
      PROGRAM PROPS
C   THIS PROGRAM DESIGNS PROPELLER BLADE CHORD AND PITCH DISTRIBUTION
C   BASED ON DUCTED FAN GEOMETRY, PERFORMANCE REQS, AND SECTION DATA.
C   IT ALSO DESIGNS THE FLOW STRAIGHTENER VANES TO MATCH PROP TORQUE.
C   OFF-DESIGN PERFORMANCE IS ALSO PREDICTED FOR RPM DIFFERENT FROM THE
C   DESIGN REQUIREMENTS AFTER THE PROPELLER BLADE IS DESIGNED.
C   FOR HIGHEST EFFICIENCY, MAXIMIZE THE GAMMAS.
      REAL K1,LETE(180)
      DIMENSION PHIM(90),BETA1(90),BETA(90),C(90),BETAV(90),CV(90)
      DIMENSION cy(90),FY(90),FX(90),TORQI(90),alph(12),cls(12)
      dimension cx(90),xlod(12)
      OPEN(UNIT=2,FILE='prop.DAT',STATUS='NEW')
      OPEN(UNIT=3,FILE='DESIG.DAT',STATUS='NEW')
C                          INPUT DATA BLOCK
C                 TREQ     = DESIGN THRUST (LBS)
C                 V0       = DESIGN FORWARD VELOCITY (FT/S)
C                 RHO      = DESIGN AIR DENSITY (SLUGS/FT3)
C                 RPI      = RADIUS OF THE PROPELLER (IN)
C                 Z        = CAMBER RATIO
C                 CL       = PROPELLER BLADE SECTIONAL LIFT COEFFICIENT
C                 GAMMA    = PROPELLER BLADE SECTIONAL LIFT/DRAG
C                 ALF      = PROPELLER BLADE SECTIONAL ANGLE OF ATTACK
C                 OMEG1    = PROPELLER DESIGN ROTATIONAL SPEED (RPM)
C                 PI       = INITIAL GUESS AT REQUIRED POWER
C                 RHI      = PROPELLER HUB RADUIS (IN)
C                 B        = NUMBER OF PROPELLER BLADES
C                 BV       = NUMBER OF STRAIGHTENER VANES
C                 K1       = PROPELLER POSITION FACTOR
C                 CLV      = STRAIGHTENER VANE SECTIONAL LIFT COEFFICIENT
C                 GAMMAV   = STRAIGHTENER VANE SECTIONAL LIFT/DRAG
C                 ALFV     = STRAIGHTENER VANE SECTIONAL ANGLE OF ATTACK
C                 CMAXI    = MAXIMUM PROPELLER ROOT CHORD LENGTH
C                 RHEI     = RADIUS OF THE EXIT HUB (IN)
C                 DTOR     = CONVERSION FACTOR FOR DEGREES TO RADIANS
C                 EXHANG   = EXIT ANGLE OF THE DIFFUSER
C                 SCORDI   = DUCT CHORD LENGTH OF ORIGINAL VEHICLE (IN)
C                 RADLI    = DUCT EXIT RADIUS OF ORIGINAL VEHICLE (IN)
C                 CVMAXI   = MAXIMUM STRAIGHTENER VANE CHORD LENGTH
C                 NZ       = NUMBER OF ANGLES OF ATTACK IN LIFT VS ANGLE
C                            OF ATTACK MATRIX FOR PROPELLER BLADE SECTIONS
C                 ALF(NZ)  = MATRIX OF ANGLES OF ATTACK FOR THE PROPELLER
C                            BLADE SECTIONS
C                 CLS(NZ)  = MATRIX OF LIFT COEFFICIENTS FOR THE PROPELLER
C                            BLADE SECTIONS
C                 XLOD(NZ) = MATRIX OF LIFT TO DRAG RATIOS FOR THE PROPELLER
C                            BLADE SECTIONS
C                 NSECT    = NUMBER OF BLADE SECTIONS
C                 IFLAG    = FLAG TO CALCULATE OFF-PERFORMANCE
      DATA TREQ,V0,RHO,RPI,Z/85.,0.,0.00192,12.0,0.1/
      DATA CL,GAMMA,ALF,OMEG1,PI,RHI/0.425,52.9,0.8,7200,26.,4.0/
      DATA B,BV,K1,CLV,GAMMV,ALFV,CMAXI/3,4,0.41,0.5,50.,0.0,3.5/
      DATA RHEI,DTOR,EXHANG,SCORDI,RADLI/4.0,0.0174533,14.0,14.5,3./
      DATA CVMAXI,nz,NSECT,IFLAG/9.5,12,90,1/
      data alph/-7.5,-5.4,-3.3,-2.2,-1.2,-0.1,0.8,3.0,5.3,7.7,8.7,10.9/
      data cls/-.287,-.109,.084,.167,.254,.342,.425,.556,.725,.845,.851,
     1      .81/
      data xlod/-3.191,-2.283,3.878,10.587,21.976,43.789,52.904,33.938,
     1         23.277,12.044,8.681,5.024/
c       data alph/-5.5,-3.5,-1.4,0.9,3.2,5.5,7.7,9.2,11.0/
c       data cls/-0.09,.109,.279,.425,.566,.709,.854,.854,.802/
c       data xlod/-1.85,5.21,24.15,47.68,31.38,19.24,12.02,7.49,5.14/
C        COVERT FROM INCHES TO FEET
      RP=RPI/12.
      RH=RHI/12.
      CMAX=CMAXI/12.
      CVMAX=CVMAXI/12.
      RHE=RHEI/12.
      RADL=RADLI/12.
      SCORD=SCORDI/12.
C        CALCULATE EXIT RADIUS, ETC., IF PROPORTIONAL TO ORIGINAL AROD
      RE=RP+RP/1.*(SCORD-RADL)*TAN(EXHANG*DTOR)
      RH=RP/3.
      S=(RP/1.*SCORD)/RE
```

```
C       CONVERT PROP SECTION AOA AND VANE SECTION AOA TO RADIANS
      ALF=ALF*DTOR
      ALFV=ALFV*DTOR
C       CONVERT RPM TO RAD/SEC
      OMEG=OMEG1*2*3.14159265/60.
C       SET INITIAL VALUES OF THRUST EXPONENT, EFFICIENCY, AND MAX
C       STRAIGHTENER VANE PITCH
      A1=1
      ETA=0.8
      THETAM=3.14159265/2.
C       CALCULATE EXPANSION RATIO AND THE PRODUCT OF THE FREE STREAM
C       DYNAMIC PRESSURE AND THE DISK AREA
      SIG=(RE**2-RHE**2)/(RP**2-RH**2)
      Q0A=0.5*RHO*V0**2*3.14159265*RP**2
      T=TREQ
C       CALCULATE TOTAL THRUST COEFFICIENT, TOTAL THRUST, AND RESET NEW CT
    5 IF(V0.NE.0.) CT=T/Q0A
      TL=CT*Q0A
      CTPN=CT
C       CALCULATE ABOVE BASED ON VELOCITY THROUGH THE PROP INSTEAD OF V0
C       IF IN HOVER
      IF(V0.NE.0.) GOTO 10
      W=SQRT(TREQ*SIG/(RHO*3.14159265*(RP**2-RH**2)))
      Q0A=0.5*RHO*W**2*3.14159265*RP**2
      CT=T/Q0A
      TL=CT*Q0A
      CTPN=CT
C       DETERMINE PROP AND SHROUD THRUST COEFFICIENTS WITH HELMBOLD'S
C       FUNCTIONS.  ALSO CALCULATE SHROUD INDUCED VELOCITY THROUGH PROP
C       IF NOT IN HOVER
   10 CTP=CTPN
      IF(V0.NE.0.) W=V0*(SQRT(1+CTP)-1)
      DELO=1.-SQRT(RE/RP)*((.458+4.431*S)/(1+1.089*S)*Z+(2.033+4.88
     1     *S)/(1+0.893*S)*S*Z**2)
      DELI=0.41*(SQRT(1+CTP)-1)
      DEL=DELO+DELI
      CTPN=CT-2*DEL*(SQRT(1+CTP)-1)
      TEST=ABS(CTPN-CTP)/CTP
      IF(TEST.GT.0.001) GOTO 10
C       CALCULATE VELOCITY THROUGH PROP AND PROP THRUST, SET PROP STRIP
C       WIDTH AND 1ST PROP STRIP NUMBER AFTER HUB
      VA=V0+W/2.+DEL*V0
      IF(V0.EQ.0.) VA=W
      TP=Q0A*CTP
      DELX=1./NSECT
      XH=RH/RP
      IXS=XH*NSECT+0.5
C       INTEGRATE THRUST AND TORQUE OVER BLADE
   15 TORQ=0.0
      THRUST=0.0
      DO 50 I=IXS,NSECT
      X=I*1./NSECT
      VTAN=PI*550./(2.*X*OMEG*RHO*VA*3.14159265*(RP**3-RH**2*RP))
      PHI=ATAN(VA/(OMEG*RP*X-VTAN))
      PHIM(I)=PHI
      CY(I)=CL*(COS(PHI)-SIN(PHI)/GAMMA)
      CX(I)=CL*(SIN(PHI)+COS(PHI)/GAMMA)
      BETA1(I)=(PHI+ALF)/dtor
      VRSQR=VA**2+(RP*X*OMEG-VTAN)**2
      IF(I.NE.IXS) GOTO 20
      DTPDX=CMAX*(B*RP*CY(I)*0.5*RHO*VRSQR)/X**A1
   20 C(I)=DTPDX*X**A1/(B*RP*CY(I)*0.5*RHO*VRSQR)
      LETE(I)=0.25*C(I)*12.
      LETE(NSECT+1-IXS+I)=-0.75*C(I)*12.
      DC=C(I)/RP
      TORQI(I)=B*C(I)*CX(I)*.5*RHO*VRSQR*RP*RP*X*DELX
      TORQ=TORQ+TORQI(I)
      FX(I)=.5*RHO*VRSQR*RP*DELX*C(I)*CX(I)
      FY(I)=.5*RHO*VRSQR*RP*DELX*C(I)*CY(I)
      THRUST=THRUST+B*C(I)*CY(I)*.5*RHO*VRSQR*RP*DELX
   50 CONTINUE
C     CALCULATE EXIT VELOCITY AND POWER AT PROPELLER PLANE
      VE=VA/SIG
      PIN=THRUST*VA/550.
C       CHECK FOR RUN-AWAY POWER VALUES
      IF(PIN.GT.500.) PIN=10.
```

```
C       RESET POWER, THRUST EXPONENT, AND CHECK FOR CONVERGENCE ON
C       PROPELLER THRUST
      PI=PIN
      A1=TP/THRUST*A1
      TEST2=ABS(TP-THRUST)/TP
      IF(TEST2.GT.0.001) GOTO 15
C       SIZE STRAIGHTENER VANES BY VANE STRIP TORQUE CANCELLING PROP
C       STRIP TORQUE AT SAME RADIAL STATION.  IF THE CENTERBODY RADIUS
C       IS LARGER THAN THE PROP HUB, TAKE THE PROP SECTIONAL TORQUES
C       WITHIN THE CENTERBODY RADIUS AND DISTRIBUTE THEM EVENLY OVER THE
C       STRAIGHTENER VANES
   55 TV=0.0
      TORQV=0.0
      SPTORQ=0.0
      XHV=RHE/RP
      IXSV=XHV*NSECT+0.5
      SPILL=1./(NSECT-IXSV)
      IF(IXS.NE.IXSV) THEN
       DO 56 I=IXS,IXSV
       SPTORQ=SPTORQ+TORQI(I)
   56  CONTINUE
      END IF
      DO 70 I=IXSV,NSECT
      X=I*1./NSECT
      VTAN=PI*550./(2.*X*OMEG*RHO*VA*3.14159265*(RP**3-RH**2*RP))
      THETA=ATAN(VTAN/VA)
      IF(THETA.LT.THETAM) THETAM=THETA
      IF(ALFV.EQ.0.) THEN
      BETAV(I)=0.0
      CLV=2*3.14159265*THETA*0.9
     * GAMMV=CLV/(1.1*(.0049*CLV**2-0.0001*CLV+0.006))
      ELSE
      BETAV(I)=(THETA-ALFV)/dtor
      END IF
      CYV=CLV*(SIN(THETA)-COS(THETA)/GAMMV)
      CXV=CLV*(COS(THETA)+SIN(THETA)/GAMMV)
      IF(I.EQ.IXSV) BETAVR=BETAV(IXSV)
      CV(I)=B*C(I)*CX(I)*(COS(THETA))**2/(BV*CXV*(SIN(PHIM(I)))**2)
      CV(I)=CV(I)+SPTORQ*SPILL*(COS(THETA))**2/(BV*CXV*.5*RHO*VA*VA*
     1 X*RP*RP*DELX)
      IF(I.EQ.IXSV) CVR=CV(IXSV)
      IF(CV(I).LT.CVMAX) GOTO 60
      BV=BV+1
      GOTO 55
   60 TV=TV+BV*CV(I)*.5*RHO*(VA/COS(THETA))**2*CYV*RP*DELX
      TORQV=TORQV+BV*CV(I)*CXV*.5*RHO*VA*VA/((COS(THETA))**2)*RP*RP*X
     1 *DELX
   70 CONTINUE
C       CHECK FOR VANE EFFICIENCY
      IF((TV.GE.0.).OR.(ALFV.EQ.0.)) GOTO 85
      PRINT 6
    6 FORMAT(1X,'VANE GAMMA INSUFFICIENT PICK ANOTHER')
      GOTO 90
   80 IF(THETAM.GE.ALFV) GOTO 85
      THETAM=THETAM/DTOR
      PRINT *,'THETA < ALFV, RERUN AT CLV AND GAMMV FOR ALFV=THETAM'
     1        ,THETAM
      STOP
C       ADD VANE THRUST AND COMPARE TO REQUIRED TOTAL THRUST.  ITERATE UNTIL
C       CONVERGED
   85 T=T+TV
      TEST3=ABS(TREQ-T)/T
C      IF(V0.EQ.0.) ETA=2./(1.+SQRT(1.+CTPN))
      IF(TEST3.LE.0.001) GOTO 90
      T=TREQ/T*(T-TV)
      GOTO 5
C       CALCULATE FINAL PERFORMANCE PARAMETERS
   90 PM=OMEG*TORQ/550.
      ETA=PIN/PM
      ETAL=2*SQRT(SIG*RHO*3.14159265*(RP**2-RH**2)/T)*550.*ETA
      CT=CTPN+2*DEL*(SQRT(1+CTPN)-1)
      CTPOCT=CTPN/CT
      TTOT=Q0A*CT
C               OUTPUT DATA BLOCK
C            CR      = PROPELLER ROOT CHORD (IN)
C            CT      = PROPELLER TIP CHORD (IN)
C            BETAR   = PROPELLER ROOT PITCH ANGLE (DEG)
C            BETAT   = PROPELLER TIP PITCH ANGLE (DEG)
```

```
C             ETA    = EFFICIENCY (THRUST POWER/TORQUE POWER)
C             ETAL   = THRUST EFFICIENCY (THRUST/POWER -- LBS/HP)
C             T      = TOTAL THRUST (LBS)
C             PTHRST = THRUST POWER (HP)
C             BV     = NUMBER OF STRAIGHTENER VANES
C             TORQ   = TORQUE PRODUCED BY PROPELLER (FT-LBS)
C             TPS    = THRUST PRODUCED BY PROP AND SHROUD
C             CVR    = VANE ROOT CHORD (IN)
C             CVT    = VANE TIP CHORD (IN)
C             BETAVR = VANE ROOT PITCH ANGLE (DEG)
C             BETAVT = VANE TIP PITCH ANGLE (DEG)
C             VA     = AXIAL AIR VELOCITY (FT/S)
C             A1     = THRUST EXPONENT
C             CTP    = PROPELLER THRUST COEFFICIENT
C             CT     = TOTAL THRUST COEFFICIENT
C             PTORQ  = TORQUE POWER (HP)
C             TORQV  = VANE TORQUE (FT-LBS)
      WRITE(3,*)'CR,CT,BETAR,BETAT,ETA,ETAL',CMAX*12.,C(NSECT)*12.,
     1      BETA1(IXS),BETA1(NSECT),ETA,ETAL
      WRITE(3,*)'T,PTHRST,BV,TORQ,TPS',T,PIN,BV,TORQ,TTOT
      WRITE(3,*)'CVR,CVT,BETAVR,BETAVT',CVR*12.,CV(NSECT)*12.,BETAVR,
     1      BETAV(NSECT)
      WRITE(3,*)'VA,A1,CTP/CT,PTORQ',VA,A1,CTPOCT,PM
      WRITE(3,*)'TORQV',TORQV
  108 format('   rpm      deltap   thrust  prop torque vane torque ',
     1      'power      eff    #/hp(ideal)')
  109 format(1x,f8.3,2x,f8.5,2x,6(f8.3,2x))
  100 CONTINUE
      WRITE(2,102)
      WRITE(2,103)
      WRITE(2,104)
  102 FORMAT(15X,'  Go 610 CIRC ARC AIRFOIL    V = 0 KTS  7200 RPM')
  103 FORMAT(1X,'    X    PROP CHORD      LE         ',
     1      'TE    VANE CHORD PROP PITCH  VANE PITCH')
  104 FORMAT(1X,'   (IN)     (IN)           (IN)          ',
     1      '(IN)       (IN)       (DEG)        (DEG)')
      DO 110 I=IXS,NSECT
      X=I*1./NSECT
      WRITE(2,105) X*RP*12.,C(I)*12.,LETE(I),LETE(NSECT+1-IXS+I),
     1            CV(I)*12.,BETA1(I),BETAV(I)
  105 FORMAT(1X,7(F8.5,3X))
  110 CONTINUE
      IF(IFLAG.EQ.0) STOP
      OPEN(UNIT=1,FILE='perfm.DAT',STATUS='NEW')
      write(1,*) '   Go 610 Airfoil Blade Designed at 7200 rpm'
      do 200 iii=1,6
      rho2=rho*(14-iii)/10.
      write(1,*) 'density=',rho2,'  slugs/cubic foot'
      write(1,108)
      do 200 i=1,17
         omeg2=omeg1+(i-9)*100.
         omeg=omeg2*2*3.14159265/60.
      do 200 ii=1,11
      delp=ii-6.
      do 300 jj=ixs,NSECT
 300  beta(jj)=betal(jj)+delp
      told=t
120   TORQ=0.0
      THRUST=0.0
      DO 250 j=IXS,NSECT
      X=j*1./NSECT
      VTAN=PI*550./(2.*X*OMEG*RHO2*VA*3.14159265*(RP**3-RH**2*RP))
      PHI=ATAN(VA/(OMEG*RP*X-VTAN))
      PHIM(j)=PHI
      alf=beta(j)*dtor-phim(j)
      alfd=alf/dtor
      call linterp(alph,cls,nz,alfd,cl)
      call linterp(alph,xlod,nz,alfd,gamma)
      CY(j)=CL*(COS(PHI)-SIN(PHI)/GAMMA)
      CX(j)=CL*(SIN(PHI)+COS(PHI)/GAMMA)
      VRSQR=VA**2+(RP*X*OMEG-VTAN)**2
      TORQI(j)=B*C(j)*.5*RHO2*VRSQR*RP*RP*X*DELX
      TORQ=TORQ+TORQI(j)
```

```
      THRUST=THRUST+B*C(j)*CY(j)*.5*RHO2*VRSQR*RP*DELX
  250 continue
      PIN=THRUST*VA/550.
      t=thrust*ct/ctp
      TV=0.0
      TORQV=0.0
      SPTORQ=0.0
      XHV=RHE/RP
      IXSV=XHV*NSECT+0.5
      SPILL=1./(NSECT-IXSV)
      IF(IXS.NE.IXSV) THEN
       DO 256 k=IXS,IXSV
       SPTORQ=SPTORQ+TORQI(k)
 256   CONTINUE
      END IF
      DO 270 j=IXSV,NSECT
      X=j*1./NSECT
      VTAN=PI*550./(2.*X*OMEG*RHO2*VA*3.14159265*(RP**3-RH**2*RP))
      THETA=ATAN(VTAN/VA)
      IF(THETA.LT.THETAM) THETAM=THETA
      CLV=2*3.14159265*THETA*0.9
      GAMMV=CLV/(1.1*(.0049*CLV**2-0.0001*CLV+0.006))
      CYV=CLV*(SIN(THETA)-COS(THETA)/GAMMV)
      CXV=CLV*(COS(THETA)+SIN(THETA)/GAMMV)
      TV=TV+BV*CV(j)*.5*RHO2*(VA/COS(THETA))**2*CYV*RP*DELX
      TORQV=TORQV+BV*CV(j)*CXV*.5*RHO2*VA*VA/((COS(THETA))**2)*RP*RP*X
     1 *DELX
 270  continue
      T=T+TV
      pi=pin
      if((abs(t-told)/told).lt.0.001) goto 230
      IF(V0.NE.0.) GOTO 220
      W=SQRT(TREQ*SIG/(RHO2*3.14159265*(RP**2-RH**2)))
      Q0A=0.5*RHO2*W**2*3.14159265*RP**2
      CT=T/Q0A
      TL=CT*Q0A
      CTPN=CT
C       DETERMINE PROP AND SHROUD THRUST COEFFICIENTS WITH HELMBOLD'S
C       FUNCTIONS.  ALSO CALCULATE SHROUD INDUCED VELOCITY THROUGH PROP
C       IF NOT IN HOVER
 220  CTP=CTPN
      IF(V0.NE.0.) W=V0*(SQRT(1+CTP)-1)
      DELO=1.-SQRT(RE/RP)*((.458+4.431*S)/(1+1.089*S)*Z+(2.033+4.88
     1      *S)/(1+0.893*S)*S*Z**2)
      if(ctp.lt.-0.99) goto 200
      DELI=0.41*(SQRT(1+CTP)-1)
      DEL=DELO+DELI
      CTPN=CT-2*DEL*(SQRT(1+CTP)-1)
      TEST=ABS(CTPN-CTP)/CTP
      IF(TEST.GT.0.0001) GOTO 220
C       CALCULATE VELOCITY THROUGH PROP AND PROP THRUST
      VA=V0+W/2.+DEL*V0
      IF(V0.EQ.0.) VA=W
      told=t
      goto 120
 230  pm=omeg*torq/550.
      eta=pin/pm
      if(t.lt.0.) goto 200
      ETAL=2*SQRT(SIG*RHO2*3.14159265*(RP**2-RH**2)/T)*550.*ETA
      write(1,109) omeg2,delp,t,torq,torqv,pm,eta,etal
  200 continue
      STOP
      END
```

B Sample Input

```
C                INPUT DATA BLOCK
C          TREQ      = DESIGN THRUST (LBS)
C          V0        = DESIGN FORWARD VELOCITY (FT/S)
C          RHO       = DESIGN AIR DENSITY (SLUGS/FT3)
C          RPI       = RADIUS OF THE PROPELLER (IN)
C          Z         = CAMBER RATIO
C          CL        = PROPELLER BLADE SECTIONAL LIFT COEFFICIENT
C          GAMMA     = PROPELLER BLADE SECTIONAL LIFT/DRAG
C          ALF       = PROPELLER BLADE SECTIONAL ANGLE OF ATTACK
C          OMEG1     = PROPELLER DESIGN ROTATIONAL SPEED (RPM)
C          PI        = INITIAL GUESS AT REQUIRED POWER
C          RHI       = PROPELLER HUB RADUIS (IN)
C          B         = NUMBER OF PROPELLER BLADES
C          BV        = NUMBER OF STRAIGHTENER VANES
C          K1        = PROPELLER POSITION FACTOR
C          CLV       = STRAIGHTENER VANE SECTIONAL LIFT COEFFICIENT
C          GAMMAV    = STRAIGHTENER VANE SECTIONAL LIFT/DRAG
C          ALFV      = STRAIGHTENER VANE SECTIONAL ANGLE OF ATTACK
C          CMAXI     = MAXIMUM PROPELLER ROOT CHORD LENGTH
C          RHEI      = RADIUS OF THE EXIT HUB (IN)
C          DTOR      = CONVERSION FACTOR FOR DEGREES TO RADIANS
C          EXHANG    = EXIT ANGLE OF THE DIFFUSER
C          SCORDI    = DUCT CHORD LENGTH OF ORIGINAL VEHICLE (IN)
C          RADLI     = DUCT EXIT RADIUS OF ORIGINAL VEHICLE (IN)
C          CVMAXI    = MAXIMUM STRAIGHTENER VANE CHORD LENGTH
C          NZ        = NUMBER OF ANGLES OF ATTACK IN LIFT VS ANGLE
C                      OF ATTACK MATRIX FOR PROPELLER BLADE SECTIONS
C          ALF(NZ)   = MATRIX OF ANGLES OF ATTACK FOR THE PROPELLER
C                      BLADE SECTIONS
C          CLS(NZ)   = MATRIX OF LIFT COEFFICIENTS FOR THE PROPELLER
C                      BLADE SECTIONS
C          XLOD(NZ)  = MATRIX OF LIFT TO DRAG RATIOS FOR THE PROPELLER
C                      BLADE SECTIONS
C          NSECT     = NUMBER OF BLADE SECTIONS
C          IFLAG     = FLAG TO CALCULATE OFF-PERFORMANCE
      DATA TREQ,V0,RHO,RPI,Z/85.,0.,0.00192,12.0,0.1/
      DATA CL,GAMMA,ALF,OMEG1,PI,RHI/0.425,52.9,0.8,7200,26.,4.0/
      DATA B,BV,K1,CLV,GAMMV,ALFV,CMAXI/3,4,0.41,0.5,50.,0.0,3.5/
      DATA RHEI,DTOR,EXHANG,SCORDI,RADLI/4.0,0.0174533,14.0,14.5,3./
      DATA CVMAXI,nz,NSECT,IFLAG/9.5,12,90,1/
      data alph/-7.5,-5.4,-3.3,-2.2,-1.2,-0.1,0.8,3.0,5.3,7.7,8.7,10.9/
      data cls/-.287,-.109,.084,.167,.254,.342,.425,.556,.725,.845,.851,
     1         .81/
      data xlod/-3.191,-2.283,3.878,10.587,21.976,43.789,52.904,33.938,
     1          23.277,12.044,8.681.5.024/
```

C Sample Output

Propeller Design Geometry

Go 610 CIRC ARC AIRFOIL V = 0 KTS 7200 RPM

X (IN)	PROP CHORD (IN)	LE (IN)	TE (IN)	VANE CHORD (IN)	PROP PITCH (DEG)	VANE PITCH (DEG)
4.00000	3.50000	0.87500	-2.62500	1.56550	35.16213	0.00000
4.13333	3.45735	0.86434	-2.59301	1.64208	34.16142	0.00000
4.26667	3.41654	0.85414	-2.56241	1.72041	33.21492	0.00000
4.40000	3.37742	0.84435	-2.53306	1.80047	32.31852	0.00000
4.53333	3.33984	0.83496	-2.50488	1.88222	31.46849	0.00000
4.66667	3.30369	0.82592	-2.47777	1.96565	30.66144	0.00000
4.80000	3.26885	0.81721	-2.45164	2.05073	29.89433	0.00000
4.93333	3.23525	0.80881	-2.42644	2.13744	29.16433	0.00000
5.06667	3.20279	0.80070	-2.40210	2.22576	28.46891	0.00000
5.20000	3.17141	0.79285	-2.37856	2.31567	27.80574	0.00000
5.33333	3.14105	0.78526	-2.35578	2.40716	27.17269	0.00000
5.46667	3.11163	0.77791	-2.33372	2.50021	26.56782	0.00000
5.60000	3.08312	0.77078	-2.31234	2.59481	25.98934	0.00000
5.73333	3.05546	0.76386	-2.29159	2.69094	25.43559	0.00000
5.86667	3.02861	0.75715	-2.27146	2.78859	24.90506	0.00000
6.00000	3.00252	0.75063	-2.25189	2.88775	24.39635	0.00000
6.13333	2.97717	0.74429	-2.23288	2.98842	23.90819	0.00000
6.26667	2.95251	0.73813	-2.21438	3.09058	23.43937	0.00000
6.40000	2.92851	0.73213	-2.19638	3.19419	22.98879	0.00000
6.53333	2.90515	0.72629	-2.17886	3.29929	22.55544	0.00000
6.66667	2.88239	0.72060	-2.16179	3.40584	22.13835	0.00000
6.80000	2.86021	0.71505	-2.14516	3.51385	21.73665	0.00000
6.93333	2.83858	0.70965	-2.12894	3.62330	21.34952	0.00000
7.06667	2.81749	0.70437	-2.11312	3.73418	20.97619	0.00000
7.20000	2.79690	0.69923	-2.09768	3.84650	20.61595	0.00000
7.33333	2.77680	0.69420	-2.08260	3.96023	20.26814	0.00000
7.46667	2.75717	0.68929	-2.06788	4.07538	19.93213	0.00000
7.60000	2.73800	0.68450	-2.05350	4.19193	19.60734	0.00000
7.73333	2.71926	0.67981	-2.03944	4.30989	19.29323	0.00000
7.86667	2.70093	0.67523	-2.02570	4.42924	18.98929	0.00000
8.00000	2.68301	0.67075	-2.01226	4.54998	18.69504	0.00000
8.13333	2.66547	0.66637	-1.99911	4.67211	18.41002	0.00000
8.26667	2.64831	0.66208	-1.98624	4.79561	18.13382	0.00000
8.40000	2.63152	0.65788	-1.97364	4.92049	17.86604	0.00000
8.53333	2.61506	0.65377	-1.96130	5.04673	17.60630	0.00000
8.66667	2.59895	0.64974	-1.94921	5.17434	17.35426	0.00000
8.80000	2.58316	0.64579	-1.93737	5.30330	17.10957	0.00000
8.93333	2.56769	0.64192	-1.92576	5.43363	16.87193	0.00000
9.06667	2.55251	0.63813	-1.91439	5.56530	16.64104	0.00000
9.20000	2.53764	0.63441	-1.90323	5.69832	16.41661	0.00000
9.33333	2.52304	0.63076	-1.89228	5.83268	16.19839	0.00000
9.46667	2.50873	0.62718	-1.88154	5.96838	15.98612	0.00000
9.60000	2.49468	0.62367	-1.87101	6.10541	15.77956	0.00000
9.73333	2.48088	0.62022	-1.86066	6.24377	15.57850	0.00000
9.86667	2.46734	0.61684	-1.85051	6.38347	15.38270	0.00000
10.00000	2.45405	0.61351	-1.84054	6.52448	15.19198	0.00000
10.13333	2.44099	0.61025	-1.83074	6.66682	15.00614	0.00000
10.26667	2.42815	0.60704	-1.82112	6.81047	14.82500	0.00000
10.40000	2.41554	0.60389	-1.81166	6.95544	14.64837	0.00000
10.53333	2.40315	0.60079	-1.80236	7.10172	14.47610	0.00000
10.66667	2.39097	0.59774	-1.79323	7.24931	14.30804	0.00000
10.80000	2.37899	0.59475	-1.78424	7.39820	14.14401	0.00000
10.93333	2.36721	0.59180	-1.77541	7.54841	13.98390	0.00000
11.06667	2.35562	0.58891	-1.76672	7.69990	13.82755	0.00000
11.20000	2.34422	0.58605	-1.75817	7.85270	13.67483	0.00000
11.33333	2.33300	0.58325	-1.74975	8.00679	13.52563	0.00000
11.46667	2.32196	0.58049	-1.74147	8.16218	13.37982	0.00000
11.60000	2.31110	0.57777	-1.73332	8.31886	13.23736	0.00000
11.73333	2.30040	0.57510	-1.72530	8.47683	13.09794	0.00000
11.86667	2.28987	0.57247	-1.71740	8.63608	12.96166	0.00000
12.00000	2.27949	0.56987	-1.70962	8.79662	12.82833	0.00000

```
C                  OUTPUT DATA BLOCK
C              CR      = PROPELLER ROOT CHORD (IN)
C              CT      = PROPELLER TIP CHORD (IN)
C              BETAR   = PROPELLER ROOT PITCH ANGLE (DEG)
C              BETAT   = PROPELLER TIP PITCH ANGLE (DEG)
C              ETA     = EFFICIENCY (THRUST POWER/TORQUE POWER)
C              ETAL    = THRUST EFFICIENCY (THRUST/POWER -- LBS/HP)
C              T       = TOTAL THRUST (LBS)
C              PTHRST  = THRUST POWER (HP)
C              BV      = NUMBER OF STRAIGHTENER VANES
C              TORQ    = TORQUE PRODUCED BY PROPELLER (FT-LBS)
C              TPS     = THRUST PRODUCED BY PROP AND SHROUD
C              CVR     = VANE ROOT CHORD (IN)
C              CVT     = VANE TIP CHORD (IN)
C              BETAVR  = VANE ROOT PITCH ANGLE (DEG)
C              BETAVT  = VANE TIP PITCH ANGLE (DEG)
C              VA      = AXIAL AIR VELOCITY (FT/S)
C              A1      = THRUST EXPONENT
C              CTP     = PROPELLER THRUST COEFFICIENT
C              CT      = TOTAL THRUST COEFFICIENT
C              PTORQ   = TORQUE POWER (HP)
C              TORQV   = VANE TORQUE (FT-LBS)
```

```
CR,CT,BETAR,BETAT,ETA,ETAL    3.500000       2.279492       35.16213
  12.82833       0.9155644       10.12396
T,PTHRST,BV,TORQ,TPS    84.99253       14.22281       8.000000       11.33178
  84.43411
CVR,CVT,BETAVR,BETAVT    1.565502       8.796620       0.0000000E+00
 0.0000000E+00
VA,A1,CTP/CT,PTORQ    159.3566       1.587530       0.5824096       15.53447
TORQV    11.33177
```

Propeller Off-Design Performance

density= 1.9200000E-03 slugs/cubic foot

rpm	deltap	thrust	prop torque	vane torque	power	eff	#/hp(ideal)
6400.000	-3.00000	3.486	2.258	-1.740	2.751	0.401	21.914
6400.000	-2.00000	17.456	3.911	2.701	4.765	0.632	15.433
6400.000	-1.00000	29.636	5.279	4.533	6.433	0.786	14.725
6400.000	0.00000	42.527	6.785	6.461	8.268	0.872	13.631
6400.000	1.00000	55.020	8.359	8.318	10.185	0.911	12.522
6400.000	2.00000	67.321	10.116	10.137	12.327	0.917	11.398
6400.000	3.00000	76.869	11.664	11.526	14.213	0.906	10.533
6400.000	4.00000	85.834	13.241	12.842	16.135	0.889	9.779
6400.000	5.00000	95.925	15.023	14.311	18.306	0.873	9.086
6500.000	-4.00000	0.163	-4.980	-3.117	-6.163	-0.021	-5.217
6500.000	-3.00000	8.577	2.794	1.336	3.458	0.438	15.245
6500.000	-2.00000	21.208	4.333	3.217	5.363	0.680	15.049
6500.000	-1.00000	34.114	5.777	5.125	7.149	0.812	14.180
6500.000	0.00000	47.220	7.291	7.051	9.023	0.886	13.138
6500.000	1.00000	60.267	8.967	8.958	11.098	0.915	12.011
6500.000	2.00000	72.230	10.704	10.696	13.247	0.915	10.973
6500.000	3.00000	81.674	12.253	12.049	15.164	0.901	10.165
6500.000	4.00000	91.077	13.899	13.404	17.201	0.884	9.439
6500.000	5.00000	101.663	15.758	14.919	19.502	0.868	8.771
6600.000	-4.00000	0.011	0.048	-2.574	0.060	1.490	1417.113
6600.000	-3.00000	12.436	3.465	1.884	4.355	0.498	14.388
6600.000	-2.00000	25.038	4.782	3.727	6.009	0.714	14.543
6600.000	-1.00000	38.764	6.296	5.723	7.912	0.832	13.628
6600.000	0.00000	51.985	7.795	7.633	9.795	0.897	12.677
6600.000	1.00000	65.725	9.593	9.608	12.055	0.917	11.529
6600.000	2.00000	77.082	11.279	11.230	14.173	0.912	10.504
6600.000	3.00000	86.526	12.845	12.562	16.141	0.896	9.821
6600.000	4.00000	96.544	14.575	13.978	18.315	0.879	9.117
6600.000	5.00000	107.563	16.508	15.531	20.744	0.862	8.473
6700.000	-4.00000	1.884	1.465	-2.189	1.869	0.340	25.289
6700.000	-3.00000	16.209	3.874	2.401	4.943	0.567	14.368
6700.000	-2.00000	29.111	5.226	4.257	6.667	0.746	14.095
6700.000	-1.00000	43.475	6.803	6.310	8.678	0.849	13.133
6700.000	0.00000	56.860	8.311	8.212	10.603	0.905	12.230
6700.000	1.00000	71.232	10.219	10.244	13.037	0.918	11.084
6700.000	2.00000	81.902	11.844	11.729	15.109	0.908	10.224
6700.000	3.00000	91.478	13.446	13.072	17.153	0.891	9.493
6700.000	4.00000	102.201	15.268	14.562	19.477	0.874	8.812
6700.000	5.00000	113.616	17.274	16.146	22.036	0.856	8.190
6800.000	-4.00000	3.981	2.398	-1.656	3.105	0.402	20.540
6800.000	-3.00000	19.940	4.242	2.896	5.492	0.625	14.271
6800.000	-2.00000	33.587	5.675	4.827	7.347	0.779	13.702
6800.000	-1.00000	48.196	7.274	6.881	9.417	0.866	12.720
6800.000	0.00000	62.000	8.872	8.811	11.486	0.909	11.773
6800.000	1.00000	76.440	10.810	10.819	13.995	0.916	10.683
6800.000	2.00000	86.724	12.403	12.228	16.058	0.903	9.889
6800.000	3.00000	96.580	14.062	13.585	18.206	0.885	9.181
6800.000	4.00000	108.039	15.976	15.153	20.685	0.869	8.523
6800.000	5.00000	119.817	18.055	16.762	23.377	0.850	7.921
6900.000	-5.00000	4.188	-23.913	-2.560	-31.416	-0.041	-2.062
6900.000	-4.00000	9.453	2.941	1.382	3.864	0.430	14.270
6900.000	-3.00000	23.747	4.650	3.386	6.109	0.667	13.953
6900.000	-2.00000	38.214	6.153	5.400	8.083	0.804	13.255
6900.000	-1.00000	52.952	7.738	7.439	10.166	0.880	12.332
6900.000	0.00000	67.448	9.473	9.434	12.445	0.912	11.318
6900.000	1.00000	81.390	11.366	11.340	14.932	0.913	10.321
6900.000	2.00000	91.636	12.968	12.723	17.037	0.899	9.573
6900.000	3.00000	101.985	14.702	14.125	19.315	0.880	8.885
6900.000	4.00000	114.041	16.699	15.749	21.939	0.864	8.249
6900.000	5.00000	126.155	18.853	17.379	24.768	0.844	7.664
7000.000	-4.00000	8.326	3.790	-0.082	5.052	0.497	17.573
7000.000	-3.00000	27.663	5.079	3.877	6.769	0.699	13.551
7000.000	-2.00000	42.942	6.649	5.970	8.862	0.822	12.791
7000.000	-1.00000	57.810	8.219	7.994	10.955	0.891	11.940
7000.000	0.00000	73.126	10.093	10.069	13.452	0.913	10.887
7000.000	1.00000	86.198	11.901	11.814	15.861	0.910	9.990
7000.000	2.00000	96.662	13.542	13.218	18.049	0.894	9.272
7000.000	3.00000	107.672	15.366	14.686	20.479	0.876	8.602
7000.000	4.00000	120.193	17.435	16.348	23.237	0.859	7.988

rpm	deltap	thrust	prop torque	vane torque	power	eff	#/hp(ideal)
7000.000	5.00000	132.520	19.652	17.983	26.192	0.838	7.421
7100.000	-5.00000	1.569	0.381	0.263	0.514	0.633	51.533
7100.000	-4.00000	17.314	4.179	2.417	5.649	0.530	12.974
7100.000	-3.00000	31.730	5.521	4.374	7.464	0.725	13.130
7100.000	-2.00000	47.767	7.153	6.536	9.669	0.837	12.342
7100.000	-1.00000	62.770	8.712	8.548	11.777	0.898	11.559
7100.000	0.00000	78.941	10.713	10.704	14.483	0.915	10.493
7100.000	1.00000	91.051	12.434	12.294	16.809	0.906	9.686
7100.000	2.00000	101.784	14.126	13.712	19.096	0.889	8.985
7100.000	3.00000	113.577	16.046	15.259	21.692	0.871	8.333
7100.000	4.00000	126.482	18.183	16.947	24.581	0.854	7.739
7100.000	5.00000	138.618	20.414	18.538	27.596	0.831	7.199
7200.000	-5.00000	3.135	1.833	-0.459	2.512	0.401	23.107
7200.000	-4.00000	21.097	4.492	2.891	6.157	0.589	13.083
7200.000	-3.00000	36.158	5.951	4.904	8.158	0.755	12.793
7200.000	-2.00000	52.606	7.621	7.087	10.447	0.852	11.970
7200.000	-1.00000	67.882	9.218	9.104	12.636	0.904	11.189
7200.000	0.00000	84.889	11.333	11.336	15.537	0.916	10.131
7200.000	1.00000	96.015	12.974	12.775	17.786	0.902	9.385
7200.000	2.00000	107.009	14.720	14.205	20.179	0.884	8.711
7200.000	3.00000	119.652	16.740	15.837	22.949	0.867	8.078
7200.000	4.00000	132.900	18.944	17.547	25.970	0.848	7.502
7200.000	5.00000	144.618	21.163	19.063	29.012	0.825	6.989
7300.000	-5.00000	8.669	2.625	1.202	3.649	0.419	14.522
7300.000	-4.00000	24.965	4.857	3.363	6.751	0.634	12.937
7300.000	-3.00000	40.827	6.387	5.450	8.877	0.781	12.468
7300.000	-2.00000	57.434	8.052	7.621	11.192	0.867	11.658
7300.000	-1.00000	73.413	9.790	9.700	13.607	0.907	10.792
7300.000	0.00000	89.670	11.840	11.784	16.456	0.912	9.822
7300.000	1.00000	101.072	13.521	13.254	18.793	0.898	9.106
7300.000	2.00000	112.337	15.326	14.697	21.302	0.878	8.448
7300.000	3.00000	125.869	17.445	16.418	24.247	0.862	7.834
7300.000	4.00000	139.431	19.718	18.145	27.407	0.843	7.276
7300.000	5.00000	150.615	21.918	19.573	30.464	0.817	6.788
7400.000	-5.00000	12.527	3.376	1.692	4.756	0.459	13.224
7400.000	-4.00000	28.943	5.252	3.836	7.400	0.669	12.674
7400.000	-3.00000	45.584	6.843	5.992	9.641	0.802	12.109
7400.000	-2.00000	62.363	8.504	8.154	11.982	0.878	11.333
7400.000	-1.00000	79.184	10.387	10.308	14.634	0.909	10.408
7400.000	0.00000	94.552	12.349	12.248	17.400	0.909	9.530
7400.000	1.00000	106.232	14.076	13.732	19.832	0.894	8.839
7400.000	2.00000	118.129	15.968	15.231	22.499	0.874	8.196
7400.000	3.00000	132.211	18.159	17.000	25.585	0.858	7.603
7400.000	4.00000	146.101	20.507	18.743	28.893	0.837	7.059
7400.000	5.00000	156.659	22.688	20.074	31.966	0.810	6.594
7500.000	-5.00000	16.486	4.017	2.181	5.737	0.497	12.485
7500.000	-4.00000	33.056	5.663	4.312	8.087	0.697	12.364
7500.000	-3.00000	50.425	7.308	6.530	10.435	0.818	11.747
7500.000	-2.00000	67.430	8.973	8.689	12.814	0.887	11.006
7500.000	-1.00000	85.037	10.978	10.910	15.677	0.910	10.057
7500.000	0.00000	99.525	12.864	12.712	18.370	0.906	9.253
7500.000	1.00000	111.492	14.638	14.210	20.904	0.889	8.585
7500.000	2.00000	124.247	16.633	15.793	23.752	0.870	7.955
7500.000	3.00000	138.663	18.883	17.581	26.965	0.853	7.382
7500.000	4.00000	152.898	21.311	19.341	30.432	0.831	6.851
7500.000	5.00000	162.773	23.478	20.571	33.527	0.802	6.404
7600.000	-5.00000	20.498	4.566	2.663	6.607	0.534	12.030
7600.000	-4.00000	37.320	6.083	4.795	8.803	0.722	12.045
7600.000	-3.00000	55.343	7.773	7.062	11.248	0.832	11.400
7600.000	-2.00000	72.654	9.460	9.228	13.689	0.893	10.682
7600.000	-1.00000	90.836	11.552	11.488	16.717	0.910	9.737
7600.000	0.00000	104.597	13.385	13.176	19.368	0.902	8.990
7600.000	1.00000	116.853	15.210	14.687	22.010	0.884	8.341
7600.000	2.00000	130.489	17.305	16.355	25.041	0.866	7.726
7600.000	3.00000	145.253	19.619	18.161	28.389	0.848	7.171
7600.000	4.00000	159.223	22.052	19.871	31.910	0.825	6.662
7600.000	5.00000	168.970	24.295	21.063	35.156	0.793	6.219
7700.000	-5.00000	24.522	5.013	3.133	7.350	0.572	11.785
7700.000	-4.00000	41.760	6.507	5.286	9.539	0.744	11.736
7700.000	-3.00000	60.329	8.234	7.589	12.071	0.844	11.077
7700.000	-2.00000	78.049	9.964	9.774	14.608	0.898	10.363
7700.000	-1.00000	96.495	12.103	12.033	17.744	0.910	9.444
7700.000	0.00000	109.768	13.911	13.639	20.395	0.898	8.739
7700.000	1.00000	122.338	15.794	15.165	23.156	0.879	8.106
7700.000	2.00000	136.839	17.985	16.917	26.368	0.862	7.508
7700.000	3.00000	151.966	20.365	18.741	29.857	0.843	6.969
7700.000	4.00000	165.363	22.772	20.361	33.385	0.818	6.486
7700.000	5.00000	175.261	25.144	21.553	36.863	0.784	6.037

rpm	deltap	thrust	prop torque	vane torque	power	eff	#/hp(ideal)
7800.000	-5.00000	28.531	5.358	3.589	7.957	0.614	11.709
7800.000	-4.00000	46.395	6.927	5.788	10.287	0.765	11.452
7800.000	-3.00000	65.387	8.682	8.110	12.894	0.855	10.783
7800.000	-2.00000	83.590	10.483	10.322	15.568	0.901	10.051
7800.000	-1.00000	101.938	12.631	12.521	18.758	0.909	9.175
7800.000	0.00000	115.037	14.444	14.101	21.451	0.894	8.500
7800.000	1.00000	128.075	16.401	15.661	24.357	0.875	7.879
7800.000	2.00000	143.322	18.674	17.479	27.733	0.857	7.300
7800.000	3.00000	158.803	21.125	19.321	31.372	0.837	6.774
7800.000	4.00000	171.571	23.506	20.846	34.909	0.811	6.314
7800.000	5.00000	181.645	26.029	22.042	38.655	0.774	5.857
7900.000	-5.00000	32.623	5.711	4.042	8.591	0.648	11.569
7900.000	-4.00000	51.224	7.344	6.300	11.046	0.786	11.189
7900.000	-3.00000	70.514	9.117	8.626	13.714	0.866	10.516
7900.000	-2.00000	89.272	11.018	10.873	16.573	0.903	9.748
7900.000	-1.00000	107.114	13.134	12.983	19.755	0.906	8.923
7900.000	0.00000	120.404	14.984	14.563	22.538	0.890	8.270
7900.000	1.00000	134.051	17.025	16.173	25.608	0.870	7.661
7900.000	2.00000	149.927	19.371	18.041	29.137	0.853	7.101
7900.000	3.00000	165.762	21.897	19.901	32.937	0.832	6.587
7900.000	4.00000	177.872	24.260	21.329	36.491	0.804	6.147
7900.000	5.00000	188.135	26.954	22.528	40.542	0.764	5.680
8000.000	-5.00000	36.822	6.087	4.496	9.272	0.677	11.366
8000.000	-4.00000	56.156	7.773	6.816	11.839	0.802	10.915
8000.000	-3.00000	75.738	9.563	9.139	14.566	0.875	10.250
8000.000	-2.00000	95.076	11.566	11.423	17.617	0.904	9.453
8000.000	-1.00000	112.271	13.633	13.430	20.766	0.903	8.684
8000.000	0.00000	125.887	15.533	15.025	23.660	0.886	8.050
8000.000	1.00000	140.259	17.665	16.700	26.907	0.866	7.453
8000.000	2.00000	156.652	20.078	18.602	30.583	0.848	6.910
8000.000	3.00000	172.610	22.654	20.456	34.507	0.826	6.412
8000.000	4.00000	184.270	25.038	21.810	38.138	0.797	5.983
8000.000	5.00000	194.691	27.925	23.012	42.536	0.753	5.504

Distribution

1510	J. W. Nunziato
1520	C. W. Peterson
1530	L. W. Davison
1550	R. C. Maydew
1551	J. K. Cole
1551	R. J. Weir (10)
1552	D. D. McBride
1553	S. McAlees, Jr.
1554	D. P. Aeschliman
1554	J. F. Henfling
1555	W. R. Barton
1556	W. L. Oberkampf
5260	J. Jacobs
5261	C. C. Hartwigsen (4)
5261	C. J. Greenholt
5261	K. D. Boultinghouse
5261	H. D. Arlowe (5)
9120	M. M. Newsom
9130	R. D. Andreas
9132	A. C. Watts
9132	J. E. White
9132	J. R. Phelan
3141	S. A. Ladenberger (5)
3151	W. L. Garner (3)

3154-1 C. H. Dalin (28) for DOE/OSTI

8024 P. W. Dean

COL R. E. Bowles, USMC
Marine Corps Development and
Education Command
Quantico, VA

Prof. J. D. Lee
The Ohio State University
Aeronautical and Astronautical
Research Laboratory
2300 West Case Rd.
Columbus, Ohio 43220

Dr. G. Boehler
Aerophysics Company
3500 Connecticut Ave N. W.
Washington, D. C. 20008

Dr. H. Chaplin
Department of the Navy
David W. Taylor Naval Ship Research and
Development Center
Carderock Laboratory
Bethesda, Maryland 20084-5000

M. Young
Department of the Navy
Naval Ocean Systems Center Code 5302
P.O. Box 997
Kailue, Hawaii 96734-0997

Prof. W. Eversman
The University of Missouri-Rolla
Department of Mechanical and Aerospace
Engineering
Rolla, Missouri 65401-0249

Prof. R. B. Oetting
The University of Missouri-Rolla
Department of Mechanical and Aerospace
Engineering
Rolla, Missouri 65401-0249